To Neal and Joyce Verhulst:
Thank you for your support.

Thanks to Charles Schuettke,
Milton Ludvigsen,
and Lawrence Verhulst.

EVALUATION AND PERFORMANCE MONITORING OF CORROSION PROTECTION PROVIDED BY FIBER-REINFORCED COMPOSITE WRAPPING

By

Stewart Mason Verhulst, B.S.

THESIS

Presented to the Department of Civil Engineering of
The University of Texas at Austin
in Partial Fulfillment
of the Requirements
for the Degree of

MASTER OF SCIENCE IN ENGINEERING

THE UNIVERSITY OF TEXAS AT AUSTIN

May, 1999

EVALUATION AND PERFORMANCE MONITORING OF CORROSION PROTECTION PROVIDED BY FIBER-REINFORCED COMPOSITE WRAPPING

APPROVED BY:

James O. Jirsa, Supervisor

David W. Fowler

Harovel G. Wheat

ACKNOWLEDGEMENTS

I thank Dr. James O. Jirsa for the help and guidance that made this report possible. His kindness and consideration are appreciated.

The support of Dr. David Fowler has made this research and my experience at The University of Texas enjoyable.

Dr. Harovel Wheat has been a great help with her knowledge and thoughtfulness.

I wish to recognize TXDOT and the efforts of Jon Kilgore, Randy Cox, Alan Kowalik, and Linda Parker. Tommy Ward of SCR Construction has been an outstanding help as well.

I express my gratitude to Paul Gugenheim of Delta Structural Technology for his considerable help and for generosity with his time, knowledge, and materials.

Dr. Moavin Islam of Concorr has been extremely gracious and receptive in his help with the equipment used for much of this project.

Jeff West has been extremely helpful, and the corrosion rate data would have been incomplete without his involvement. Much thanks to him.

The staff of Ferguson Structural Engineering Laboratory is excellent and has been outstanding in their help with the considerable labor involved in this research. Special thanks go to Peter Joyce and Eric Matsumoto for their insight.

This project could not have been completed without the staff of the Construction Materials Research Group. Michael Rung and Gordon Shepperd have been especially helpful and my thanks goes to them.

Finally, I thank my research partner Laura Fuentes for her friendship and for an outstanding working relationship. Best wishes to her and the future so bright ahead.

Stewart Mason Verhulst
Austin, TX
May 7,1999

EVALUATION AND PERFORMANCE MONITORING OF CORROSION PROTECTION PROVIDED BY FIBER-REINFORCED COMPOSITE WRAPPING

Stewart Mason Verhulst, M.S.E.
The University of Texas at Austin, 1999

Supervising Professor: Dr. James O. Jirsa

Corrosion damage of reinforced concrete structures has become an extremely costly maintenance item in the United States. The structures affected are commonly those in or near marine environments and transportation structures on which de-icing salts are used. An increasingly popular repair method for structures in corrosive environments is the application of a fiber-reinforced composite wrap to the concrete surface. The objective of this report is to establish a field research program to analyze the effects of composite wrapping systems on the corrosion process. The research includes performance monitoring with various devices to help determine corrosion conditions before and after repair with a wrapping system.

TABLE OF CONTENTS

LIST OF TABLES

LIST OF FIGURES

Chapter 1

PROJECT 1774 OVERVIEW

1.1 Effect of FRP Composite Wrapping on Reinforced Concrete Structures

Fiber Reinforced Plastic (FRP) composite materials have been used for years as a method of providing added strength and ductility to reinforced concrete structures. The conventional FRP system is a fabric saturated with an epoxy resin, which is "wrapped" in layers around the concrete surface. FRP wrapping has been most widely used in applications where seismic actions pose a threat to the strength and deformation capacity of an existing structure.

In recent years, FRP composite wrapping has been considered and implemented (on a few projects) for corrosion protection. Corrosion due to chloride ingress is purportedly arrested by the prevention of further chloride contamination and penetration by the oxygen and water needed to continue a corrosion process that has begun or has caused damage. Figure 1.1 shows a structure that has been repaired with a composite wrapping system.

Figure 1.1 Structure wrapped with FRP.

1.1.1 Chloride Contaminated Concrete

Many questions remain about the effectiveness of FRP wrapping for corrosion protection, especially in repair conditions where the concrete has already been contaminated with chlorides. In these cases, only the damaged concrete is removed and replaced prior to wrapping, effectively trapping the chlorides in the remaining section inside the sealed concrete member. For the purposes of investigating the effect of this condition, both a laboratory research program and a field research program have been implemented. The laboratory program includes control specimens which contain no chlorides prior to wrapping.

1.2 Literature Review

Much of what has been done in both the laboratory program and in the field research program is based on, or is an extension of, previous studies. A literature search was conducted to understand the process of corrosion and its effects on reinforced concrete members. The search was focussed on previous laboratory and field research involving the use of FRP wrapping for corrosion protection.

It is also important to understand the techniques underlying different types of monitoring equipment – especially the corrosion rate devices used in this study. Each device operates differently, making it necessary to understand these differences for the purpose of data interpretation. The manual for each device was the primary resource for this information.

1.3 Field Research Program

A program for field research and performance monitoring has been established and is the focus of this report. The purpose is to assess the condition of actual structures in a corrosive environment. The structures are to be repaired and wrapped with FRP composites and evaluated both before and after this repair.

1.3.1 State Highway Project CSR 783-2-66 in Lubbock, TX

The structures being studied in the field research program are bridge

overpass substructures located in and around Lubbock, TX and Slaton, TX. These structures have been subjected to a corrosive environment in the presence of chlorides. This has led to corrosion of the reinforcing steel and spalling and delamination of the concrete cover in areas where the chlorides were allowed to concentrate, as shown in Figure 1.2. Due to the extent of the damage, a project involving repair and FRP wrapping to shield out all further chlorides was begun. In conjunction with this project, some data collection before and after the repair was necessary to evaluate the effectiveness of this repair method.

1.3.1.1 Condition Prior to Construction

To characterize the condition of the structural elements before Project CSR 783-2-66 began, a number of field tests were carried out. These tests included visual inspection, corrosion rate measurement, chloride content testing, and concrete permeability testing. Tests were performed at selected locations with the exception of visual inspection, which was performed at each structure designated for repair.

Figure 1.2 Typical Corrosion Damage on Project CSR 783-2-66.

1.3.1.2 Performance Monitoring in Service

The corrosion rate testing mentioned in 1.3.1.1 gives valuable information on structural conditions, but the corrosion rate values are only valid for the moment that the measurement is taken. Because of this, it is necessary to take readings incrementally over time to achieve an accurate portrayal of the corrosion-related performance of the repair.

Conventional field corrosion rate measurement equipment requires access to both the concrete surface and the steel reinforcement. This is not possible on Project CSR 783-2-66 because of the presence of the external wrap. In addition, it is also preferable to test non-destructively, not by removing concrete cover to achieve a connection to the reinforcement.

The solution is to use permanent corrosion rate probes, which are embedded into the repair material and are electrically connected to the reinforcement. Embedded probes take the place of the field testing equipment and can be used to take measurements at any time. Embedded probes are used on this project for long-term evaluation of the corrosion activity. Measurements are to be taken regularly, as outlined in Chapter 5.

1.3.2 Evaluation of Monitoring Equipment

Another part of the field research is the evaluation of the monitoring equipment itself. The equipment was used on the recommendation of the Texas Department of Transportation based on products outlined by the Federal Highway Administration (FHWA) in the Strategic Highway Research Program (SHRP).

In addition to the embedded probes, three field devices were used for corrosion rate measurement. Two of the field devices were used on large laboratory beam specimens as well as on the structures in Lubbock. In this way, a better comparison and characterization of the devices can be made.

The field permeability equipment was compared against the standard ASTM test for concrete permeability: ASTM C 1202-94. Correlation between these measurements was made.

The accuracy of the testing equipment was also evaluated by cross-referencing the values obtained from different tests. For example, high chloride contents are compared with the relative corrosion rate values at that location. Permeability values might be compared with the chloride depth profile. Some correlation of this nature is expected.

1.4 Laboratory Research Program

A complement to the field research is a laboratory experimental program. The purpose of the laboratory program is to simulate field conditions and investigate the effects of a number of parameters considered important for corrosion control. Specimens are to be exposed to an accelerated corrosive environment while closely representing conditions observed in actual structures. During exposure, the specimens are to be continually monitored so that the effects of each parameter over time can be assessed. At the end of the study, each specimen will be autopsied and closely inspected to determine the level of corrosion damage and the condition of the specimen. More detailed information on the laboratory program can be found in Appendix G.

Chapter 1

PROJECT 1774 OVERVIEW

1.1 Effect of FRP Composite Wrapping on Reinforced Concrete Structures

Fiber Reinforced Plastic (FRP) composite materials have been used for years as a method of providing added strength and ductility to reinforced concrete structures. The conventional FRP system is a fabric saturated with an epoxy resin, which is “wrapped” in layers around the concrete surface. FRP wrapping has been most widely used in applications where seismic actions pose a threat to the strength and deformation capacity of an existing structure.

In recent years, FRP composite wrapping has been considered and implemented (on a few projects) for corrosion protection. Corrosion due to chloride ingress is purportedly arrested by the prevention of further chloride contamination and penetration by the oxygen and water needed to continue a corrosion process that has begun or has caused damage. Figure 1.1 shows a structure that has been repair with a composite wrapping system.

Figure 1.1 Structure wrapped with FRP.

1.1.1 Chloride Contaminated Concrete

Many questions remain about the effectiveness of FRP wrapping for corrosion protection, especially in repair conditions where the concrete has already been contaminated with chlorides. In these cases only the damaged concrete is removed and replaced prior to wrapping, effectively trapping the

chlorides in the remaining section inside the sealed concrete member. For the purposes of investigating the effect of this condition, both a laboratory research program and a field research program have been implemented. The laboratory program includes control specimens which contain no chlorides prior to wrapping.

1.2 Literature Review

Much of what has been done in both the laboratory program and in the field research program is based on, or is an extension of, previous studies. A literature search was conducted to understand the process of corrosion and its effects on reinforced concrete members. The search was focussed on previous laboratory and field research involving the use of FRP wrapping for corrosion protection.

It is also important to understand the techniques underlying different types of monitoring equipment – especially the corrosion rate devices. Each device operates differently, making it necessary to understand these differences for the purpose of data interpretation. The manual for each device was the primary resource for this information.

1.3 Field Research Program

A program for field research and performance monitoring has been established and is the focus of this report. The purpose is to assess the condition of actual structures in a corrosive environment. The structures are to be repaired

and wrapped with FRP composites and evaluated both before and after this repair.

1.3.1 State Highway Project CSR 783-2-66 in Lubbock, TX

The structures being studied in the field research program are bridge overpass substructures located in and around Lubbock, TX and Slaton, TX. These structures have been subjected to a corrosive environment in the presence of chlorides. This has led to corrosion of the reinforcing steel and spalling and delamination of the concrete cover in areas where the chlorides were allowed to concentrate, as shown in Figure 1.2. Due to the extent of the damage, a project involving repair and FRP wrapping to shield out all further chlorides was begun. In conjunction with this project, some data collection before and after the repair was necessary to evaluate the effectiveness of this repair method.

1.3.1.1 Condition Prior to Construction

To characterize the condition of the structural elements before Project CSR 783-2-66 began, a number of field tests were carried out. These tests included visual inspection, corrosion rate measurement, chloride content testing, and concrete permeability testing. Tests were performed at selected locations with the exception of visual inspection, which was performed at each structure designated for repair.

Figure 1.2 Typical Corrosion Damage on Project CSR 783-2-66.

1.3.1.2 Performance Monitoring in Service

The corrosion rate testing mentioned in 1.4.1.1 gives valuable information on structural conditions, but the corrosion rate values are only valid for the moment that the measurement is taken. Because of this, it is necessary to take readings incrementally over time to achieve an accurate portrayal of the corrosion-related performance of the repair.

Conventional field corrosion rate measurement equipment requires access to both the concrete surface and the steel reinforcement. This is not possible on Project CSR 783-2-66 because of the presence of the external wrap. In addition, it is also preferable to test non-destructively; not by removing concrete cover to achieve a connection to the reinforcement.

The solution is to use permanent corrosion rate probes, which are embedded into the repair material and are electrically connected to the reinforcement. Embedded probes take the place of the field testing equipment and can be used to take measurements at any time. Embedded probes are used on this project for long-term evaluation of the corrosion activity. Measurements are to be taken regularly, as outlined in Chapter 5.

1.3.2 Evaluation of Monitoring Equipment

Another part of the field research is the evaluation of the monitoring equipment itself. The equipment was used on the recommendation of the Texas Department of Transportation based on products outlined by the Federal Highway Administration (FHWA) in the Strategic Highway Research Program (SHRP).

In addition to the embedded probes, three field devices were used for corrosion rate measurement. Two of the field devices were used on large laboratory beam specimens as well as on the structures in Lubbock. In this way, a better comparison and characterization of the devices can be made.

The field permeability equipment was compared against the standard ASTM test for concrete permeability – ASTM C 1202-94. Correlation between these measurements was evaluated.

The accuracy of the testing equipment was also evaluated by cross-referencing the values obtained from different tests. For example, high chloride contents are compared with the relative corrosion rate values at that location. Permeability values might be compared with the chloride depth profile. Some correlation of this nature is expected.

1.4 Laboratory Research Program

A complement to the field research is a laboratory experimental program. The purpose of the laboratory program is to simulate field conditions and investigate the effects of a number of parameters considered important for corrosion control. The specimens are to be exposed to an accelerated corrosive environment while closely representing conditions observed in actual structures. During exposure, the specimens are to be continually monitored so that the effects of each parameter over time can be assessed. At the end of the study, each specimen will be autopsied and closely inspected to determine the level of corrosion damage and the condition of the specimen. More detailed information on the laboratory program can be found in Appendix G.

Chapter 2

CORROSION OF STEEL IN A CONCRETE ENVIRONMENT

2.1 The Corrosion Process

Corrosion has increasingly become a structural problem the world over. Structures in and around marine environments and transportation structures exposed to deicing salts are especially at risk. Of specific interest are reinforced concrete structures, in which the steel is hidden inside the members and is therefore not easily visually inspected. Corrosion of steel in concrete is an electrochemical process. This process is triggered when the surface of the reinforcing steel becomes depassivated, allowing the steel to be oxidized in the presence of water and oxygen.

Concrete is alkaline by nature with a pH value of about 12.5. This provides a protective environment, helping to insure that the reinforcement does not corrode (Hausmann 1965). A thin passive film, or layer, composed of gamma iron oxide is created on the steel surface (Hime and Erlin 1987). This layer prevents corrosion from taking place and is well maintained in the alkaline environment of the concrete. It is when this layer breaks down that corrosion can begin. Black steel has been found to depassivate in concrete environments at values around pH 11.5 (Yeomans 1991).

As an electrochemical process, corrosion involves the transfer of electrons as a result of chemical reactions. This requires an anode and a cathode.

The anode is the site of the oxidation of the steel. The reaction at the anode is expressed as:

$$Fe \rightarrow Fe^{2+} + 2e^{-} \qquad [2.1].$$

The liberated electrons are used at the cathode – the site of the reduction reaction:

$$2e^{-} + H_2O + \tfrac{1}{2} O_2 \rightarrow 2OH^{-} \qquad [2.2].$$

With the corrosion process underway, the reinforcing steel oxidizes to form ferric oxide (Fe_2O_3) or rust. This can be expressed by the following series of equations and is outlined in Figure 2.1 (Broomfield 1997):

$$Fe^{2+} + 2OH^{-} \rightarrow Fe(OH)_2 \qquad [2.3]$$

$$4Fe(OH)_2 + O_2 + 2H_2O \rightarrow 4Fe(OH)_3 \qquad [2.4]$$

$$2Fe(OH)_3 \rightarrow Fe_2O_3 \bullet H_2O + 2H_2O \qquad [2.5].$$

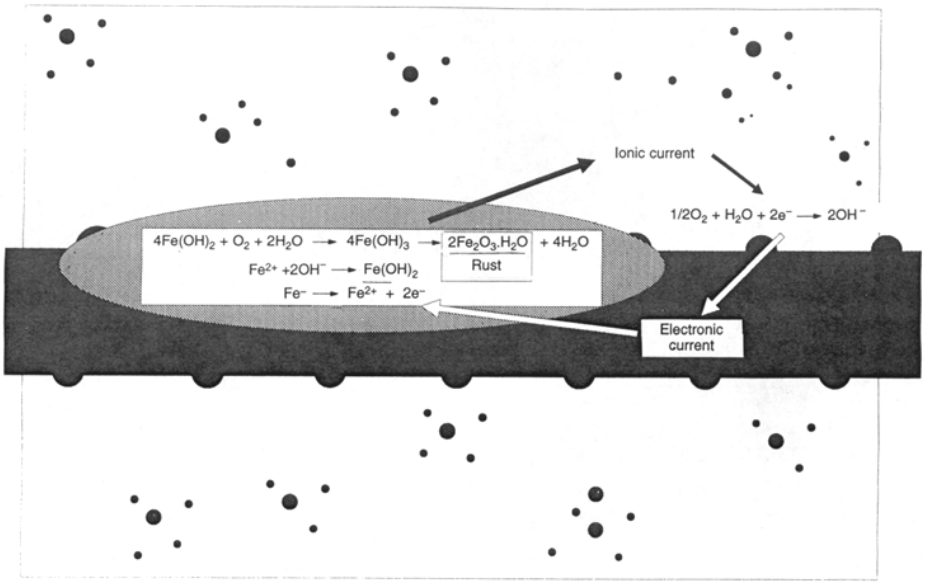

Figure 2.1 Corrosion reactions and rust formation on the steel surface (Broomfield 1997).

The formation of rust is the most tangible evidence of corrosion and causes many of the problems associated with corrosion damage in reinforced concrete. Hydrated ferric oxide ($Fe_2O_3 \bullet H_2O$) may have up to ten times the volume of the consumed steel that it replaces (Broomfield 1997). This substantial volumetric increase causes pressures in the concrete, which leads to cracking and spalling of the concrete cover. While spalling is primarily a serviceability issue, delamination at the steel/concrete interface and reduction of the cross-sectional area of the reinforcement can compromise structural integrity.

2.2 Causes of Corrosion in Reinforced Concrete

Corrosion, or oxidation of the reinforcing steel, in concrete occurs when the local environment becomes such that the steel loses its passivity. There are two major causes of corrosion damage to reinforced concrete structures: carbonation and chloride ion penetration.

Corrosion Due to Carbonation

Carbonation is defined as "The process by which carbon dioxide in the atmosphere reacts with water in the concrete pores to form a carbonic acid and then reacts with the alkalis in the pores, neutralizing them" (Broomfield 1997). Carbonation migrates to the reinforcing steel, causing pH reduction and breakdown of the passive layer. Alkalinity may drop as low as pH 8 in carbonated regions, much lower than the value required for depassivation.

The mechanism of carbonation is basically diffusion of the carbonated pore water into the concrete. Therefore, the parameters which influence corrosion by carbonation are invariably those which affect the depth and rate of diffusion. Such parameters include the amount of concrete cover and the concrete permeability. Permeability is a function of water-cement ratio and fine aggregate content. The correlation between permeability and carbonation is evident in cracked specimens. Carbonation will proceed quickly along the crack with little penetration into the concrete perpendicular to the crack surface (Francois and Arliguie 1991).

Corrosion Due to Chloride Ion Penetration

Much of the corrosion evident in reinforced concrete structures is due to chloride ion penetration. Chloride ions migrate through the concrete matrix, reaching the steel reinforcement and breaking down the passive layer. The destruction of the passive film in the presence of chlorides is due more to localized concentrations of free chloride ions, as shown in Figure 2.2, than to the reduction in pH at the bar surface.

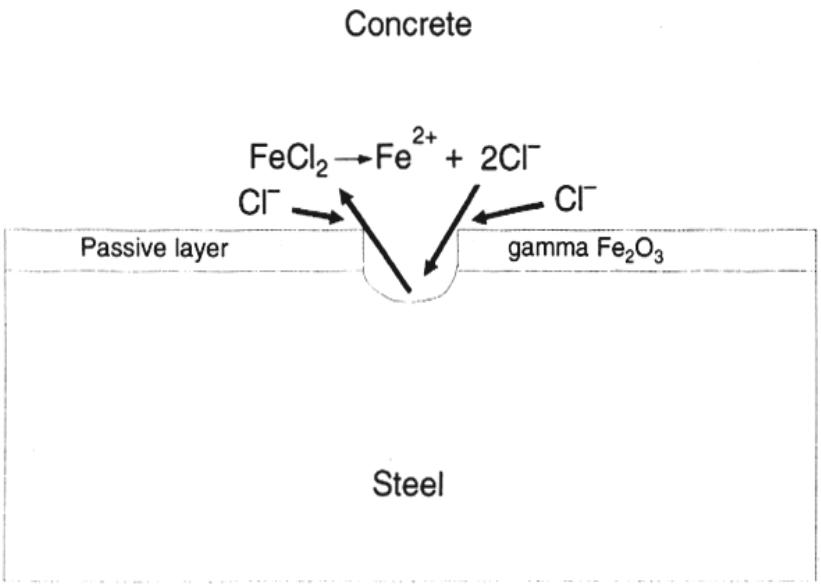

Figure 2.2 Termination of the passive layer by chloride ions (Broomfield 1997).

There are many sources of chlorides for corrosion of steel in concrete. The two main classifications are chlorides cast into the mix and chlorides which diffuse into the concrete during service exposure. Some sources of chlorides cast into the mix include (Broomfield 1997):

- Chloride set accelerators
- Use of sea water during mixing

- Contamination of aggregates.

Examples of chloride diffusion sources include (Broomfield 1997):

- Marine environment splash and spray
- Use of deicing salts on transportation structures
- Chemical application or storage.

The amount of chlorides required to induce corrosion is very difficult to measure, but is usually expressed as a percentage of concrete weight. Critical chloride percentages are 0.4 percent by weight if they are cast into the mix and 0.2 percent if they enter the concrete by diffusion (Broomfield 1997). Once corrosion has begun, free chlorides can react with corrosion products to reduce the alkalinity of the immediate area, further enhancing the corrosion process (ACI Committee 222 1991, Fraczek 1987). Since chloride ion penetration is a diffusion process, many of the influencing parameters are the same as for carbonation. The amount of concrete cover has a large effect on the ability of reinforcement to avoid chloride attack. Chloride ion penetration is also sensitive to the surrounding environment. The most corrosive environment is cyclic wetting and drying (Mirsa and Uomoto 1991), an environment that allows access into the concrete for both water-borne chlorides and oxygen.

The amount and proximity of flexural cracking has a considerable effect on corrosion. Localized corrosion is accelerated at the point of the crack. When enough corrosion has taken place to initiate longitudinal cracking, corrosion spreads along the reinforcement. It is evident that the amount of cover and cracking are dependent on one another. Cracking may dominate short-term corrosion characteristics, but adequate cover and the spacing of cracks may have

more significant effects on the long-term corrosion performance of a structure (Mirsa and Uomoto 1991).

In the vast majority of structures, chloride ion ingress is much more critical than carbonation. Corrosion due solely to carbonation is only expected where concrete cover is exceptionally low or in environments with severe carbon dioxide concentrations. However, lower amounts of carbonization may accelerate the corrosion process through interaction with chloride ion penetration. If carbonization depassivates the protective surface film, the corrosion due to the concentrated free chlorides can proceed more easily. Experimental results indicate that carbonization amplifies corrosion for a given chloride content, although high chloride concentrations in the concrete matrix may slow the carbonation rate (Roper and Baweja 1991).

2.3 Common Methods for Corrosion Repair and Prevention

If the amount of corrosion in a structure is (or is expected to be) substantial, it is likely that some repair or prevention technique is necessary to mitigate the corrosive effect. There are many techniques, both physical and electrochemical, to delay initial or to slow existing corrosion activity. The application of a surface coating or sealer is one repair method that is intended to create a barrier to the incoming contaminated water, thereby robbing corrosion of its reactants (Broomfield 1997). Unfortunately, there is still some question about the reliability of waterproofing using these treatments.

The use of coated reinforcement is a widely used technique for corrosion prevention. The two most common examples are epoxy coated reinforcement

and galvanized reinforcement. Fusion-bonded epoxy is intended to prevent corrosive elements from reaching the steel surface. Concern arises when the epoxy layer is damaged during transport or installation. If kept intact, epoxy coatings are effective for corrosion prevention (Yeomans 1991).

Galvanized reinforcement provides corrosion protection in two ways. The zinc galvanized layer on the steel surface acts as a barrier to chlorides. Zinc also corrodes in a sacrificial manner in relation to steel reinforcement, protecting locations where the layer has been damaged or broken down. The zinc coating remains passive at pH values around 9.5, much lower than the threshold for unprotected steel (Yeomans 1991). Galvanized reinforcement is most effective in situations with low or moderate chloride exposure.

Electrochemical repair methods attempt to take advantage of the inherent electrochemistry of the corrosion process to help reduce or prevent further corrosion. Popular electrochemical techniques include cathodic protection and chloride removal.

Cathodic protection is essentially the polarization of a metal to reduce the corrosion rate. An electrode is connected electrically with the reinforcement. This electrode becomes the anode, forcing the steel to become the cathode; halting the corrosion process (Jones 1996).

Chloride removal (or extraction) also involves polarization of the reinforcement. An electrode applies current to the steel, driving it to a more negative potential. The negatively charged chloride ions are repelled from the steel surface and are attracted to the positive anode. While cathodic protection is

often a permanent or long-term technique, electrochemical chloride removal is temporary and uses higher impressed current densities (Vaca 1993).

Some practical corrosion prevention methods are reduction of concrete permeability and pore water through the addition of an admixture and changing structural drainage characteristics to prevent chloride contamination at critical sections. For a given exposure environment, the presence of adequate cover is an important factor in long-term durability (Swamy 1990).

2.4 Corrosion Protection Provided by FRP Wrapping Systems

FRP wrapping systems have been used extensively in seismic retrofits and for structural maintenance. Many of the maintenance applications depend on the external wrap to prevent further chloride ingress and therefore halt the corrosion process inside the structure.

The results of past research have raised questions regarding the effectiveness of FRP wrap and jacket systems to prevent ongoing corrosion (Sohanghpurwala and Scannell 1994 and Unal and Jirsa 1998). The field research involves repaired structures which have undergone some corrosion. The corrosion behavior of previously unexposed (new) reinforced concrete structures treated with an FRP wrapping system has not been thoroughly evaluated and is an integral portion of the laboratory program.

Chapter 3

PREVIOUS AND CURRENT USES OF FRP WRAPPING SYSTEMS

3.1 Introduction to FRP Systems

Fiber Reinforced Plastic (FRP) composites are a relatively new group of materials in structural engineering applications. FRP products are also called Advanced Composite Materials (ACM) in existing literature. The term "composite" refers to the combination of two materials to form one effective system. In the case of FRP, the materials involved are generally a high-strength fiber-reinforced material and a polymer resin.

FRP materials are often used to provide structural strength and have enjoyed widespread use on transportation structures. Many of the highway structures in the United States and around the world were built following World War II. In the US, the interstate highway program structures built in the 1950's and 60's are approaching or exceeding their design life. These structures have now aged and the initial design strengths have been exceeded by current traffic demands (Mufti, Erki, and Jaeger 1991).

FRP may be the most appropriate material for strengthening and repair of reinforced concrete structures in many situations. FRP is a very durable material and is especially effective in marine or salt environments, as it is corrosion resistant. FRP also has a high strength-to-weight ratio, making it easier to handle and install than conventional strengthening materials (such as steel or concrete jackets). Use of FRP has been limited by its relatively high cost and by a lack of

familiarity in the construction and engineering communities (Mufti, Erki, and Jaeger 1991). However, with increasing availability of reliable data from laboratory testing and field application, FRP will become more widely accepted, and high material costs may be offset by the reduced construction time, ease of application, and non-interruption of use of the structure.

The most common strengthening techniques using FRP materials include:

- Prestressing tendons
- Plates on the tension face of the concrete
- Circumferential wrapping of the concrete element.

The use of prestressing tendons is primarily for new construction and seems to be effective, although some durability concerns remain (Mufti, Erki, and Jaeger 1991). FRP bonded plates and wrapping systems have also been used effectively and will be discussed in this chapter.

The fibers used in FRP composites are generally either glass or carbon based. Glass fibers are much cheaper to produce and are more widely used. Carbon fibers are much stronger than glass and can create stiffer elements with less material. Carbon fibers should not be used in a corrosion protection wrapping system. The carbon may form a galvanic corrosion cell with the reinforcement, causing the steel to act anodically and preferentially corrode. Consequently, glass fiber fabrics were used for both the laboratory and field programs in this study.

The polymer material used to complete the composite matrix and bond the fabric to the concrete surface and subsequent layers of fabric is usually an epoxy resin. This material protects the fibers and helps prevent cracking and

fiber separation (Neale and Labossiere 1991). The use of a vinyl-ester material in the laboratory program illustrates the importance of choosing a polymer compatible with the fiber-reinforced fabric. The vinyl-ester promoted fabric breakdown, making wrap installation difficult. Many polymer materials are subject to degradation with continued exposure to ultraviolet (UV) light and must be protected by a surface coating.

3.2 The Tyfo® S Fibrwrap® System

The Tyfo® S Fibrwrap® composite wrapping system is the primary FRP system in both the laboratory and field research programs. Fibrwrap® is used for member strengthening and as corrosion protection in repair situations and in new construction. The Fibrwrap® system can be applied with either glass fabric or carbon fiber. Although both may be used for strengthening, the carbon fiber is considerably stronger and stiffer. Because the Fibrwrap® system is applied in layers, use of the carbon fiber reduces the amount of labor required for installation and allows a lower repair thickness (Delta Structural Technology 1998). Glass fabric is used in applications where reinforcement corrosion is a concern because the objective is to provide a reliable barrier that will have a long service life. The carbon and glass reinforced materials are shown in Figures 3.1 and 3.2 respectively. More information on material properties can be found in Appendix A.

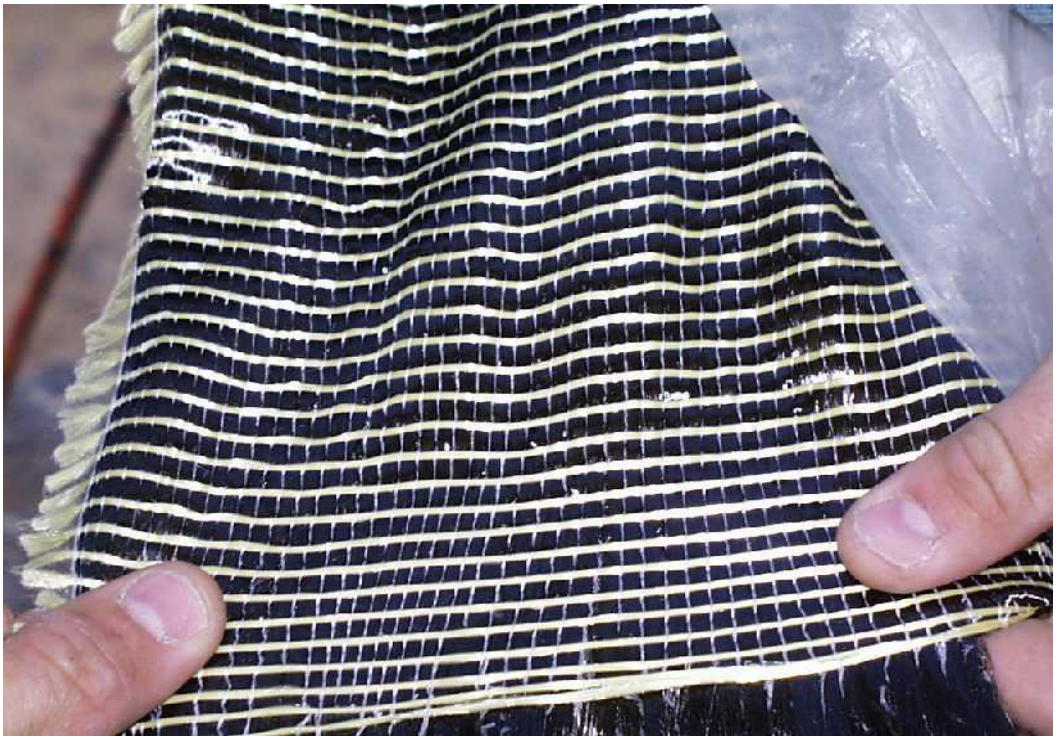

Figure 3.1 Tyfo® S Fibrwrap® carbon fiber reinforced fabric.

Figure 3.2 Tyfo® S Fibrwrap® primary glass fabric.

Some of the advantages of the Fibrwrap® system for repair are:

- Increased shear and flexural strength of columns,
- Increased column ductility,
- Durability in corrosive environments,
- System confines corrosion stresses and prevents further chloride ingress,
- System can be applied to virtually all geometric shapes.

The Tyfo® S Fibrwrap® systems have also been used to provide flexural strength in beams and slabs in place of methods such as steel-plate bonding (Delta Structural Technology 1998).

Other proprietary composite wrapping systems have been used to enhance the performance of reinforced concrete structures. A system marketed by XXsys Technologies, Inc. is a carbon composite jacket and is used to add strength and ductility to concrete members – especially columns. The applications of this system are primarily seismic retrofit situations. An automated system is used to apply the wrap to typical column elements (XXsys Technologies 1998).

3.3 Laboratory Testing Involving FRP Composites

Much of the laboratory research involving FRP composite materials is investigation of the added strength supplied to reinforced concrete. This strength is commonly provided either by use of bonded plates or by wrapping.

Experiments show that glass FRP plates, when applied to the tension face of reinforced concrete members, increased the flexural load capacity and reduced

both crack formation and crack width at all load levels. Strength gains provided by FRP plates are most pronounced for members with lower reinforcement ratios (Saadatmanesh and Ehsani 1996). Further research indicates increases in stiffness, yield moment, and ultimate moment; as well as a reduction in curvature when epoxy-bonded FRP composite plates are used (Saadatmanesh, Ehsani, and An 1996).

Epoxy-bonded composites have some advantages over epoxy-bonded steel plates for use as strength repair. In moist or corrosive environments corrosion may occur at the steel-epoxy interface causing a critical reduction in the bond strength, diminishing composite action on the tension face. Composites are not susceptible to corrosion. FRP sections are also much lighter than the steel required to achieve equivalent strength levels, allowing faster and easier installation. This is especially important in situations where the structure must be kept in service during repair (Saadatmanesh, Ehsani, and An 1996).

A study supported by the Florida Department of Transportation (FDOT) in which the shear strength and confinement provided by FRP jackets filled with concrete were investigated. The FRP jackets did not bond sufficiently with the concrete to give substantial gains in shear strength. However, when shear connectors were provided, the members acted as composite sections and displayed large gains in shear strength. Axial loading tests showed that FRP developed more confinement in circular sections than in rectangular sections (Mirmiran 1997).

Laboratory testing of the Tyfo® S Fibrwrap® systems shows increased strength and ductility in repaired reinforced concrete members. Experiments using the glass fabric system on concrete joist sections and beam-column elements illustrated the ductility supplied by wrapping. Another test performed on a column element showed that the wrap increased the ductility factor from 1 to 8 (McConnell 1993). The Fibrwrap® system outperformed steel jacketing retrofits in many situations (Delta Structural Technology 1998).

In comparison with the studies on FRP strengthening, research on the use of FRP composites for corrosion protection is limited. Composite wrapping is an attractive repair method for corrosion damaged reinforced concrete elements for two reasons: (1) the wrap forms a physical barrier to the ingress of oxygen, water, and water-borne chlorides; and (2) wrapping provides confinement of the section under expansive pressures from the corrosion process (Sheikh, et. al). It should be noted that a wrapped member has better confinement characteristics than the FRP jacketed members in the FDOT study because of superior bonding to the concrete surface.

Sheikh, et. al investigated corrosion damaged specimens repaired with the Tyfo® S Fibrwrap® glass fabric system. The results showed that the columns repaired with the FRP system regained their original strength and had significantly increased ductility (Sheikh, et.al).

The corrosion process in reinforced concrete members encapsulated and injected with an epoxy resin was studied by Unal (Unal and Jirsa 1998). Both encapsulated and control specimens were included in the study and each specimen contained both uncoated (black) reinforcement and epoxy-coated bars.

After exposure to a saltwater environment, the corrosion of the black reinforcement in the encapsulated specimens was more severe than in the control specimens. Pitting corrosion was also observed near the beam ends of the encapsulated specimens. Water discovered at inlet holes of the encapsulation system (for corrosion potential testing) was determined to have originated from inside the specimens. This is the result of capillary leaching action in the encapsulated concrete. Core testing showed little or no epoxy penetration into the concrete matrix. In general, while water and chlorides did not penetrate the glass fiber system, the corrosive elements remaining in the specimens at the time of encapsulation were trapped inside. The encapsulation did not arrest corrosion in the encapsulated specimens over the length of the study.

3.4 Field Applications of FRP Composite Wrapping Systems

FRP composite wrapping systems have been used extensively in structural applications in the last decade. These applications are primarily for repair and strengthening of reinforced concrete elements. Protection against further corrosion has been presumed for some repair conditions in marine environments.

3.4.1 FRP for Seismic Strengthening

The initial use of FRP composite wrapping systems was for seismic retrofit strengthening and ductility enhancement. The laboratory performance of FRP is encouraging, but the importance lies in structural behavior under actual seismic loading. During the magnitude 6.6 Northridge Earthquake of 1994, reinforced concrete columns wrapped with FRP remained standing and showed

no visible damage. Columns repaired with steel jacketing also performed well during the quake (Buzbee 1994, Civil Engineering 1994). The construction process of applying FRP wrap is much more efficient and is less disruptive than the procedure for providing steel jacketing (Civil Engineering 1994).

3.4.2 FRP for Corrosion Repair and Maintenance

In addition to seismic applications, FRP composite wrapping systems have been used widely for maintenance repairs, especially for damage due to reinforcement corrosion. The Wisconsin DOT has used the Tyfo® S Fibrwrap® system for maintenance of column elements. All such applications performed successfully and further use is planned (Okpala 1996). The Fibrwrap® system is also being used and evaluated on the delaminated columns of a bridge spanning FDR Drive in New York.

Although FRP wraps clearly provide added strength when used as repairs, they have not been as successful for prevention of corrosion in previously exposed elements. The conventional methods of removing damaged concrete and replacing it with a repair material are insufficient in severe environments (such as marine environments). Consequently, FRP jackets have been applied to the splash zone of submerged reinforced concrete piles to prevent the ingress of corrosive elements. However, capillary action in the concrete matrix supplied moisture and chlorides from below the waterline and allowed oxygen to migrate from above the wrapped section. The wrapped section may have actually suffered accelerated corrosion as the concrete was not allowed to dry and corrosive elements in the section prior to the repair were not allowed to escape

(Sohanghpurwala and Scannell 1994). These results are similar to those observed in laboratory exposures (Unal and Jirsa 1998).

Chapter 4

FRP PROTECTION IN PROJECT CSR 783-2-66

4.1 Outline of Construction Methods

The scope of Project CSR 783-2-66 is to repair and/or replace bridge bent endcaps and substructures which have sustained extensive corrosion damage. After the repair of the existing structures is finished, a FRP composite wrapping system is to be applied externally to protect against future corrosion. The primary construction duties on Project CSR 783-2-66 are handled by SCR Construction Company, Inc. of Texas. The wrapping of the repaired structures is being done by Delta Structural Technology, Inc.

4.1.1 Removal and Repair of Concrete Surface

Figures 4.1 and 4.2 show typical corrosion damage to bent endcaps. The project specifications call for cover removal back to sound concrete for the damaged portions of the downstream endcaps. The reinforcement is to be cleaned and/or replaced as necessary to remove all previous corrosion products. Welding of the reinforcing steel is not permitted on this project. Figure 4.3 shows an endcap with the steel exposed and the preparations made for repair. During the period of structural repair, the structures are supported and bridges are not open to traffic.

The repair material used is Shotpatch® 21F, a material made by Master Builders Technologies®, Inc. The specifications of this material are listed in

Appendix B, and call for the surface to be cleaned of all materials that would interfere with the bond to the sound concrete substrate (Master Builders Technologies 1999).

Figure 4.1 Endcap damage to Structure #5.

Figure 4.2 Closeup of corrosion damage on Structure #8.

Figure 4.3 Endcap prepared for application of repair material on Structure #3.

Shotpatch® 21F is applied by a shotcrete process. This application and the temporary formwork are shown in Figure 4.4. Figure 4.5 illustrates a typical endcap after the formwork has been removed. It is evident that the concrete cover was removed to just inside the outer column face at this particular location (Structure #3).

Figure 4.4 Application of Shotpatch® 21F to Structure #3.

Figure 4.5 Endcap repair material on Structure #3.

4.1.2 Application of TYFO® S Fibrwrap® Wrapping System

Delta Structural Technology, Inc. uses TYFO® S Fibrwrap® to protect and add strength to reinforced concrete columns. The wrapping done on Project CSR 783-2-66 involves epoxy resin saturated into a glass fabric. The specifications for this material can be found in Appendix A.

Prior to placement of the composite material, the concrete surface must be prepared to provide the necessary bond characteristics and to prevent the development of air pockets beneath the wrap.

The first step of the preparation is spraying the surface to be wrapped with a corrosion inhibitor. The product approved for Project 783-2-66 is Sherwin Williams® Macropoxy 920 Pre-Prime. The surface is then ground smooth, to expunge any protrusions which may cause voids, and is cleaned to provide a fresh surface. Before the saturated fiber is applied, the surface is coated with a layer of epoxy to enhance uniform bond.

The mechanism used to provide saturated fabric is displayed in Figure 4.6. The epoxy is in effect rolled into the fabric. Once the fabric is saturated, it is applied to the substructure. Figure 4.7 shows the wrap being placed on an endcap of Structure #2. Three layers of wrap are applied in succession, to prevent polymerization of the previous layer. This ensures complete bonding between layers.

After each layer is placed, any air pockets (or “bubbles”) must be removed by rubbing. This is a major construction concern and the process is

demonstrated in Figure 4.8. About 24 hours after the final layer is applied, the entire surface is painted with a high-solids paint to provide UV protection for the wrapping system and to match the color to that of the existing structure. An example of a finished and painted endcap is shown in Figure 4.9. The Fibrwrap® system can be applied at a rate of about 2 bents in 2 days on skewed bridges, and a little faster on structures with more orthogonal geometry.

Figure 4.6 Saturation machine used by Delta Structural Technology, Inc.

Figure 4.7 Application of Fibrwrap® to endcap on Structure #2.

Figure 4.8 Removal of air pockets beneath a layer of Fibrwrap®.

Figure 4.9 Wrapped and painted endcap on Structure #2.

Chapter 5

PERFORMANCE MONITORING ON PROJECT CSR 783-2-66

5.1 Evaluation Prior to Repair

The city of Lubbock is located in Northwest Texas, just south of the panhandle. It has a population of 222,636 and is located at latitude 33.6N, longitude 101.8W (United States Census Bureau 1999). The climate in this part of northern Texas includes some freezing periods, during which deicing salts must be used on the roadways. The result is a corrosive environment for bridge decks and substructures.

5.1.1 Forensic Review of Structural Conditions

Many of the corrosion-related problems on the structures being repaired for Project CSR 783-2-66 occur on the low or "downstream" end, toward which all water and water-borne particles are drained. Of particular concern are the end sections on the substructure bridge bents. Many of the downstream end portions of these bents have experienced severe cracking, delamination, and spalling, as shown in Figures 5.1 and 5.2.

Figure 5.1 Corrosion damage on downstream endcap.

Figure 5.2 Closeup of area with severe concrete spalling.

Just as the substructure beams show distress in the areas subjected to drain water, the columns in the drainage path exhibited cracking and delamination. Figure 5.3 shows the damage on one such column located on structure #3, at the interchange of US Highways 62 and 82 and Loop 289.

Figure 5.3 Concrete spalling on a bridge support column.

There is also some delamination evident on the top portion of the substructure bents near the center and downstream supports, where water drains along the deck beams.

In addition to the visual inspection, the structural conditions were evaluated on a quantitative basis using equipment and methods recommended by the FHWA. The tests performed include corrosion rate measurement, concrete permeability measurement, and chloride content determination. A cross-comparison between data gathered from these tests and from the visual evaluation yields a more accurate assessment of the corrosion damage.

5.1.2 Corrosion Rate Measurements

There are different methods used to quantify the process of corrosion in concrete environments. The most widely used method is probably half-cell potential measurement, using either a saturated calomel electrode or a copper-copper sulfate electrode (CSE). While half-cell potentials have been shown to give the probability of corrosion occurrence and can be traced over time to show trends, they do not give any indication of the dynamic effect of the corrosion process (Scannell, Sohanghpurwala, and Islam 1996). Consequently, there is an effort to develop systems which can accurately measure the corrosion rate and help to predict remaining structural serviceability.

Three systems recommended by FHWA were used in the corrosion rate evaluation of the overpass substructures in Lubbock: the 3LP device, the PR-Monitor, and the Gecor device. These systems are covered in more detail in Chapter 6. The results from all three devices are shown in Table 5.1.

Table 5.1 Corrosion Rate Measurement Data on Project CSR 783-2-66.

	Location (Structure #)					
	#8	**#7**	**#1**	**#5**	**#10**	**#11**
3LP						
Ecorr (mv vs. CSE)	-40	N/A	-100	-270	N/A	-157
Icorr ($\mu A/cm^2$)	0.1347	N/A	0.0431	0.063	N/A	0.6207
PR-Monitor						
Ecorr (mv vs. CSE)	-108	-79.2	-102.7	-74.9	-66.8	-144.5
Icorr ($\mu A/cm^2$)	0.0219	0.46	0.0044	0.018	0.15	0.302
Rate (mpy)	0.01	0.21	0.002	0.008	0.069	0.138
Gecor						
Ecorr (mv vs. CSE)	-83.8	-78.3	-116.4	-41.4	-49.8	-113
Icorr ($\mu A/cm^2$)	0.01	0.001	0.009	0.003	0.008	0.022
Interpretation	Passive	Passive	Passive	Passive	Passive	Passive

Table 5.1 shows the corrosion potentials as measured by each device. The 3LP device was somewhat inconsistent in this limited number of samples. This could be due to the use of an aging CSE pencil electrode and the corresponding difficulty in filling the electrode with a properly saturated $CuSO_4$ solution. It is likely that the low 3LP potential value on Structure #8 and the high value on Structure #5 are erroneous.

The PR-Monitor and Gecor device provided similar corrosion potential measurements as shown in Figure 5.4. The higher the corrosion potential, the more negative are the values. There may be error in some readings from each device due to the difficulty of applying the electrode sponges to vertical surfaces with limited overhead clearance. However, all of the readings were greater than

–200 mv vs. CSE, which indicates a low probability of corrosion according to ASTM C 876 (ASTM).

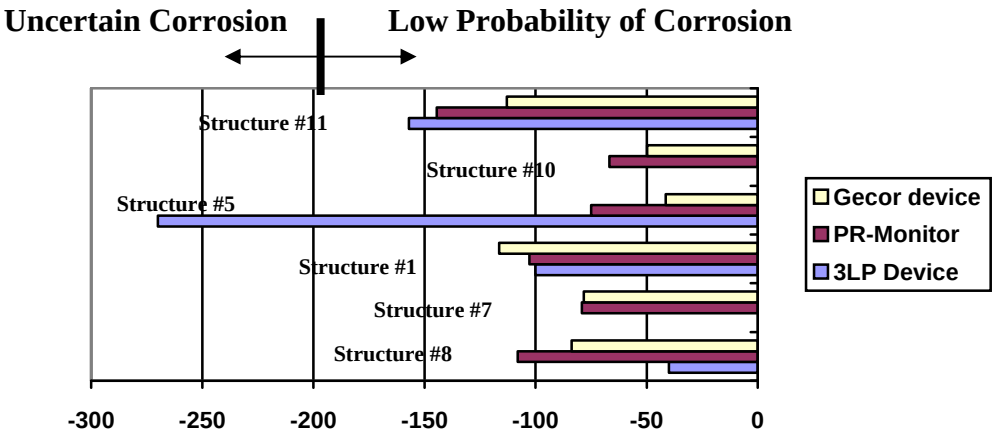

Figure 5.4 Corrosion Potential (mV vs. CSE) values from different equipment.

Each of the devices also gives a value of current density, shown in Figure 5.5. There is large disparity between the output values from each device. Table 5.2 gives some guidelines for corrosion rate evaluation (Scannell, Sohanghpurwala, and Islam 1996).

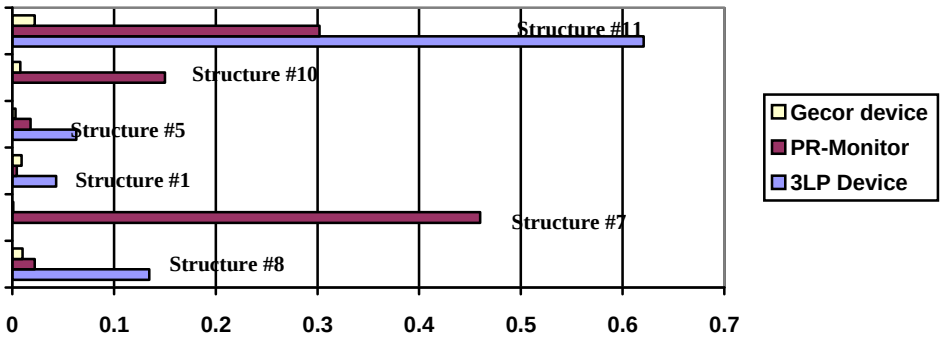

Figure 5.5 Corrosion current density ($\mu A/cm^2$) values from different equipment.

Table 5.2 Guidelines for data interpretation corrosion rate devices (Scannell, Sohanghpurwala, and Islam 1996).

3LP Device

- Icorr less than 0.20 mA/ft^2 (0.186 μA/cm^2)
  - No corrosion damage expected.
- Icorr between 0.20 and 1.0 mA/ft^2 (0.186and 0.929 μA/cm^2)
  - Corrosion damage possible in 10 to 15 years.
- Icorr between 1.0 and 10 mA/ft^2 (0.929 and 9.29 μA/cm^2)
  - Damage expected in 2 to 10 years.
- Icorr in excess of 10 mA/ft^2 (9.29μA/cm^2)
  - Corrosion damage expected in 2 years or less.

PR-Monitor and Gecor Devices

- Icorr less than 0.1 μA/cm^2
  - Passive condition.
- Icorr between 0.1 and 0.5 μA/cm^2
  - Low corrosion rate.
- Icorr between 0.5 and 1.0 μA/cm^2
  - Moderate corrosion rate.
- Icorr in excess of 1.0 μA/cm^2
  - High corrosion rate.

While it is not likely that these data can be used quantitatively, relatively high rates of corrosion on Structures #7, 8, 10, and 11 are predicted. The PR-Monitor yields corrosion current values indicating some corrosion in Structures

#7, 10, and 11, while the 3LP device detects significant corrosion activity in each of the structures on which it was used (1, 5, 8, and11).

The corrosion rate measurements were not taken on the end cap of the bents where the corrosion damage was obviously the most severe. To provide a good connection to the reinforcement, accessed from coring, as well as to avoid delaminated sections, measurements were taken 10-20 feet from the downstream end of the bent. In these regions, the corrosion rate is not expected to be as high as for the obviously damaged sections and therefore the corrosion rate data from the 3LP device and the PR-Monitor seem reasonable.

The presence of delaminations, such as those shown on Structure #10 in Figure 5.6, made the corrosion rate device difficult to stabilize in some areas. This is because of a high solution resistance caused by the discontinuous medium between the working electrode and the reference electrode.

Figure 5.6 Delaminations and corrosion stains on a downstream endcap.

It is necessary that corrosion rate testing with each of these devices be controlled and carefully done. Ideally, a number of tests should be run on a given structural element to provide a better comparison. This could be done more easily with an external attachment to the steel, such as a lead wire from inside the element, eliminating the destructive nature of the tests.

More information on the corrosion rate evaluations at each location is contained in the corrosion rate data sheets, located in Appendix C.

5.1.3 Chloride Content Determination

Measurement of the chloride content in the bridge substructures on Project CSR 783-2-66 is another way to classify the possibility of corrosion. Table 5.3 shows the chloride percentages in the different structures and at different distances from the downstream ends of the bents.

The chloride content measurements were taken from concrete at a depth of ½ in. to disregard any surface imperfections or inconsistencies. Samples were taken in three ½-in. increments from three different drill-holes at each location to provide enough concrete dust for the analysis. The drill used was a rotary hammer drill with a ¾-in. hammer bit.

To collect the samples efficiently from the vertical surfaces without contamination, the dust was pulled by a vacuum through coffee filters. The samples were stored in plastic zip-lock bags immediately following collection.

A commonly used chloride threshold for corrosion is 1lb. chloride per cubic yard of concrete, or about 0.026 percent chlorides by weight (Broomfield 1997). Based on this value, many of the locations tested on Project CSR 783-2-66 are considered probable sites for active corrosion. With the reinforcement at a cover depth of approximately 2.5 in., determined by a reinforcement locator (pachometer), the chloride content at the level of the steel will be somewhat less than the values in Table 5.3. However, these values give an indication of the chloride concentration profile at each sample location and many of the values are sufficiently high to expect corrosion at greater depths.

Table 5.3 Chloride percentages by concrete weight for Project CSR 783-2-66.

	Depth (in.)		
Location	**0.5 – 1.0**	**1.0 – 1.5**	**1.5 – 2.0**
Structure #8 – 10 feet from the	0.12	0.034	0.0038
Structure #8 – 2.5 feet from the	0.17	0.21	0.20
Structure #7 – 20 feet from the	0.19	0.18	0.15
Structure #7 – 12 feet from the	0.21	0.28	0.16
Structure #3 – 22 feet above the ground	0.26	0.29	0.19
Structure #2 – 17 feet from the	0.31	0.22	0.16
Structure #2 – 25 feet from the downstream end (left of center column).	0.056	0.08	0.042
Structure #1 – Directly on the downstream	0.01	0.0056	0.003
Structure #5 – Directly on the spalled downstream end-cap.	0.45	0.38	0.21
Structure #5 – 10 feet from the downstream end (some spalling present).	0.082	0.043	0.0035
Structure #10 – Between columns away	0.003	0.003	0.003
Structure #11 – On the top of the bent.	0.018	0.02	0.018

Chloride contents and corrosion rate values correlate well. Both Structure #7 and Structure #8 show relatively high chloride contents near the downstream ends and also yielded significant corrosion rates. It is noteworthy that it was difficult to stabilize the corrosion rate devices at many locations of high chloride content, such as on Structures #2 and #7. This is due to the presence of subsurface delaminations, as mentioned in section 5.1.2. These delaminations are evidence of significant corrosion activity.

The chloride sample data sheets contain detailed information on the tests performed and can be found in Appendix D.

5.1.4 Permeability Testing

To obtain information on the concrete quality and how it may be contributing to the corrosion-related deterioration on Project CSR 783-2-66, permeability characteristics were measured. Permeability testing was done by two methods: rapid permeability testing of extracted cores and the use of a motorized Surface Air Flow (SAF) device.

The cores were drilled with a 4-in. nominal diameter and then cut to thicknesses of 2 in. before being subjected to electrical current according to ASTM C 1202-94. They were then evaluated for chloride ion penetrability based on the amount of charge passed through the sections (ASTM 1994). An example of a core sample (prior to cutting) taken from Structure #10 is shown in Figure 5.7.

Figure 5.7 Permeability core taken from Structure #10.

The SAF device is based on the flow of air at the concrete surface under a vacuum. The device was developed under SHRP project C-101, and measures the permeability of the concrete to a depth of about ½ in. (Scannell, Sohanghpurwala, and Islam 1996).

The permeability data collected in Lubbock are displayed in Table 5.4. The permeability sample data sheets can be found in Appendix E. The chloride ion penetrability is evaluated based on Table 1 in ASTM C 1202-94 (ASTM 1994). The SAF results are assessed with respect to the guidelines contained in Table 5.5.

There seems to be only limited correlation between the ASTM method and the SAF device. They both indicate high permeability of Structure #2

(where severe delamination prevented corrosion rate determinations), and both suggest high permeabilities for the majority of the samples. However, beyond this the numbers are inconsistent. The values from the SAF device in particular seem very high.

Table 5.4 Concrete permeability measurements for Project CSR 783-2-66.

	SAF Device		**ASTM Permeability**	
Location	Flow Rate (ml/minute)	Relative Permeability	Charge (C)	Ion Penetrability
Structure #2	97.45	High	10930	High
Structure #7	71.08	High	1630	Low
Structure #8	18.51	High	5600	High
Structure #10	43.5	High	5200	High

Table 5.5 Relative permeabilities for the SAF device (Scannell, Sohanghpurwala, and Islam 1996).

Air Flow Rate (ml/minute)	**Relative Permeability Category**
Less than 5	Low
Between 5 and 16	Moderate
Greater than 16	High

The flow rate values generated by the SAF device may be affected by an inability of the particular equipment used to generate the proper vacuum. The calibration protocol calls for a stable value between 750 and 765 mm Hg (Scannell, Sohanghpurwala, and Islam 1996). The device used could not develop a vacuum above about 685 mm Hg.

Based on visible corrosion damage, the concrete permeability for the structures in Project 783-2-66 is expected to be rather high. More samples are

necessary for an accurate determination of the permeability, but the destructive nature of coring on the bridge substructure limited the testing to four locations. However, this restricted sampling does suggest that the concrete is relatively permeable, and it is evident that chlorides have penetrated the cover and reached the reinforcing steel.

5.2 Continued Performance Monitoring in Service

While the tests described in section 5.1 are important to establish the structural conditions prior to repair, they give no information on what will happen after the structures are repaired and wrapped. Evaluation of conditions in service is necessary to gauge the effectiveness of the wrapping system as a corrosion prevention technique.

The Fibrwrap® system used on project CSR 783-2-66 is an external application and prevents contact with the concrete surface. Contact is required for all of the field corrosion rate measurements, as is electrical contact with the reinforcement. Therefore, the performance of field corrosion rate tests on wrapped structures would necessitate removal of the wrap at test locations. The tests would also demand either the installation of lead-wire connections to the reinforcement during the repair process, or core drilling to achieve electrical contact during the test. In effect, portable field corrosion rate tests would be destructive and could compromise the integrity of the wrapping system at locations where the environment was most corrosive. A non-destructive corrosion rate measurement technique was required.

5.2.1 Embedded Corrosion Rate Probes

To avoid destructive testing, embedded corrosion rate probes were installed during the repair construction process. These probes are manufactured by Concorr, Inc. and are discussed in more detail in Chapter 6.

5.2.1.1 Probe Installation

The embedded probes were installed after the damaged concrete was removed. After a location was selected, the probe was placed and oriented to allow current flow from the counter electrode to the reinforcement under evaluation. In Project CSR 783-2-66, probes were placed next to the longitudinal reinforcement and are connected electrically to the reinforcement cage (working electrode).

An electrical connection was established by means of silver soldering the copper ground wire from the probe to the reinforcement. To prepare the steel surface for the soldering procedure, the surface was ground as shown in Figure 5.8. Once a length of about 1 to 2 in. of bright steel was produced, a cleaning agent (flux) was applied to all surfaces and the copper ground wire was placed in contact with the steel reinforcement.

The soldering was done with an oxy-acetylene torch. Due to the restricted access to the locations of probe installation, a torch much smaller than a standard welding torch was required. This torch consisted of an oxygen tank, an acetylene tank, and the gas hoses and adjustable nozzle. Protective eyewear and gloves had to be worn when using the torch.

To operate the torch for soldering, first the oxygen valve was opened and the flame was started with a striker. The flame was adjusted to the point where no black smoke was emitted. The acetylene was then added to the flame until a small, defined inner cone of flame was achieved near the nozzle as shown in Figure 5.9. The flame was applied to the steel and copper attempting to keep the tip of the inner cone, which was the hottest part of the flame, on the surface as shown in Figure 5.10. When the metals at the interface were sufficiently heated and the flux had melted and cleaned the surfaces, the silver solder was applied to the junction between the copper and steel. A connection of about 1 in. was provided to prevent detachment during subsequent construction. A 56 percent silver solder alloy was used for all probe installations and is recommended for connecting copper and steel.

Figure 5.8 Grinding of the reinforcement to prepare for soldering.

Figure 5.9 Torch flame for solder application.

Figure 5.10 Application of flame to the copper-steel interface.

Figure 5.11 shows a typical finished soldered connection. The probe is installed some distance away from the solder point to prevent the erroneous measurement of corrosion due to the other metals and the heat-treated steel. Figure 5.12 displays a fully installed embedded corrosion rate probe.

Figure 5.11 Typical silver soldered electrical connection.

Figure 5.12 Installed probe on Structure #7.

Two probes were installed on Structure #7 and four were installed on Structure #8. The installations are recorded in Table 5.5. In many cases the endcaps were already repaired at the time of installation, leaving limited space for placement of the embedded probes. This was the case on Structure #8, where all probes are installed in sections about 4 feet from the downstream end of the bent.

The designation (left or right) in Table 5.6 is from the perspective of someone looking at the structure from the downstream end. For reference, the direction of traffic is from left to right.

The area of steel polarized by the probes is essentially the surface area of the portion of the bar receiving current from the probe. This area is calculated as

the circumference of each reinforcing bar facing the counter electrode times the 5-in. length of the probe.

Table 5.6 Probe installation locations.

ID #	Structure	Beam Face	Distance from End (ft.)	Steel Area (in^2)
7.1	#7	Left	7.5	44.30
7.2	#7	Right	4	44.30
8.1	#8	Left	4	44.30
8.2	#8	Right	4	44.30
8.3	#8	Left	4	44.30
8.4	#8	Right	4	22.15

5.2.1.2 Corrosion Rate Measurements

The corrosion rate measurements from the embedded probes will be taken using the PR-Monitor corrosion rate measurement device. The probes are equipped with a connection cable containing wires from the reference, counter, and working electrodes. The cables are about 20 feet in length and reach out of the structure for the future monitoring. There is a six-pin connector at the end of the cable for connection with the PR-Monitor.

To protect against vandalism and the elements, the end of the connection cable was placed in a junction box in a location not accessible to the public. A lift will be required to take measurements with the PR-Monitor, which weighs about 20 lbs.

5.2.2 Plan for Long-Term Evaluation

The measurements taken with the PR-Monitor give information on the corrosion potential and corrosion rate. These values are only valid for the time of the test, requiring a repeated test schedule for accurate long-term evaluation. In another application with these same embedded probes, readings were taken every three months. Due to the long life-expectancy of the repaired structures, however, a six-month test interval would be more appropriate. The tests may be run by University of Texas representatives continuing work on the project or by Texas Department of Transportation personnel. The automated nature of the PR-Monitor device makes the test procedure straightforward and repeatable.

Chapter 6

EVALUATION OF PERFORMANCE MONITORING EQUIPMENT

6.1 Introduction to Equipment and Usage

An important part of the research conducted in the field on Project CSR 783-2-66 was the use and evaluation of the performance monitoring equipment provided or recommended by the Texas Department of Transportation. The purpose was to determine the usefulness and accuracy of the different types of equipment and compare results with currently used methods. The equipment includes corrosion rate measurement devices, a field chloride content determination kit, and an instrument for the field estimation of concrete permeability.

There were four corrosion rate measurement devices evaluated for field effectiveness. Three of these are for portable, quick, nondestructive testing: the 3LP device, the PR-Monitor, and the Gecor device. The fourth corrosion rate device is an embedded probe for long-term, in-service corrosion rate measurement. These devices use variations of the concept of linear polarization to collect data and to determine the corrosion rate.

6.1.1 Linear Polarization

The linear polarization method, or polarization resistance method, is an electrochemical method for determining corrosion rate. Polarization is defined as the potential change in a metal due to a change in electron flow, and therefore a

change in the reaction rates, at the corroding surface. For corrosion rate determinations, an applied current is generally used to change the flow of electrons. Linear polarization has become a rather widely used method because of the ease and efficiency of the testing. In comparison with standard weight-loss testing, linear polarization takes a fraction of the time and is both non-destructive and repeatable. This allows more versatile and continuous use in engineering and/or quality control applications (Jones 1996).

The concept of linear polarization has spawned a number of portable instruments for in-service testing, such as the four corrosion rate devices used in this study. There are two common probe types for linear polarization measurement: two-electrode probes and three-electrode probes.

The linear polarization method takes its name from the apparent linearity of polarization curves near their origin. This is the region of low applied current and subsequently low overvoltages (voltages differing from the determined corrosion potential, Ecorr). Figure 6.1 shows a hypothetical polarization curve in both the anodic and cathodic regions. Note that the region of curve linearity is limited to points near the origin. For this reason, the linear polarization method is commonly referred to as the "polarization resistance" method, with polarization resistance defined as the slope of the polarization curve at the origin (Jones 1996).

The values β_a and β_c are known as the Tafel constants (anodic and cathodic respectively) and are determined by the relationships in Equations 6.1 and 6.2:

$$\varepsilon_c = \beta_c \log i_c/i_{corr} \qquad [6.1]$$

$$\varepsilon_a = \beta_a \log i_a/i_{corr} \qquad [6.2].$$

ε_c and ε_a are the cathodic and anodic overvoltages and i_c and i_a are the current densities applied during the polarization (Jones 1996).

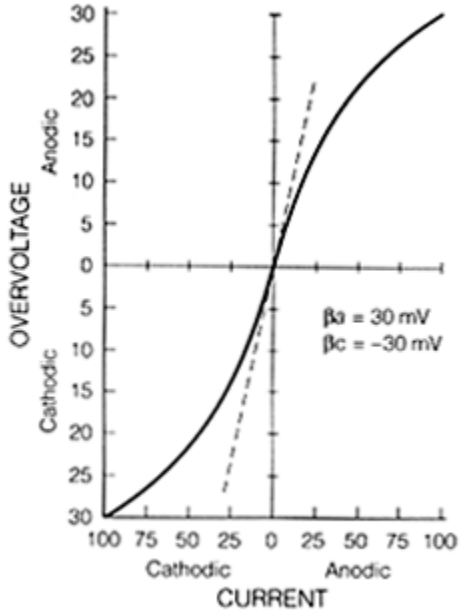

Figure 6.1 Hypothetical anodic and cathodic polarization curves (Jones 1996).

Polarization resistance,R_p, is determined by the relationship in Equation 6.3:

$$R_p = [\Delta e/\Delta i_{app}]_{e\to 0} = B/i_{corr} \qquad [6.3].$$

B is the proportionality constant, as defined in Equation 6.4, which is also known as the Stern-Geary Equation (Jones 1996, Kenneth C. Clear 1990):

$$B = \beta_a\beta_c / 2.3 (\beta_a + \beta_c) \qquad [6.4].$$

For concrete, the values of B range from about 26 to 52 mV depending on the steel passivity (Broomfield 1997). Errors in the estimation of the Tafel constants will not egregiously affect the corrosion rate determination. With arbitrary values, the error is limited to a factor of about two, and the error is significantly reduced if there is a Tafel constant determination of even limited accuracy (Jones 1996).

An important element to remember when calculating the polarization resistance for concrete is the effect of the solution resistance, R_s. For most applications of polarization resistance, the solution resistance is negligible and is ignored when calculating the actual polarization resistance. However, for mediums with large values of solution resistance (such as concrete), the measured polarization resistance will be much larger than the actual value of R_p. This will cause an erroneously low corrosion rate reading (Cortest).

Polarization resistance techniques have other inherent limitations which must be considered. The corrosion rate determination is an instantaneous test and gives only the value of the rate at that particular time. For an accurate measurement of the deterioration caused by corrosion, the rate should be taken at intervals over a period of time. In addition, the area of steel that is effectively polarized may be difficult to calculate due to "fanning" of the applied polarization current and/or the close spacing of subsequent layers of reinforcement (Broomfield 1997). Such situations can be corrected if the characteristics of the polarization equipment are known. Temperature and relative humidity also have an effect on corrosion rate values but can arguably be

ignored due to the relatively large rate differences between active and passive steel (Scannell, Sohanghpurwala, and Islam 1996).

There are two distinct instrumentation methods for polarization resistance: galvanostatic and potentiodynamic. Galvanostatic methods involve the application of polarizing currents in a step-by-step fashion. Potentiodynamic testing is similar, except overvoltages are applied in steps. Both are steady-state methods. Galvanostatic instrumentation enjoys wider use in conventional corrosion rate measurement equipment. Potentiodynamic methods may be subject to problems involving corrosion potential drift that makes an accurate measurement difficult to obtain (Jones 1996).

Polarization resistance, or linear polarization, appears to be the preferred method for measuring the corrosion rate of steel reinforcement. Some transient methods have been evaluated as well, but certain obstacles cannot be overcome. The NSC device uses the AC impedance method and was originally to be included in the FHWA-SHRP Showcase, but it was difficult to obtain and, more importantly, the time required for testing was inconvenient for field applications (Scannell, Sohanghpurwala, and Islam 1996). Other transient methods have encountered similar problems and also fail to account for changing variables over the period of the test (Jones 1996). Consequently, polarization resistance will likely remain the method of choice, and efforts will be concentrated on enhancing accuracy of measurement so that quantitative results are more reliable.

6.1.2 Description of Testing Environments

The SHRP equipment was evaluated both in the laboratory and in the

field. The field testing was conducted on corrosion damaged bridge overpass elements in Lubbock, TX and is discussed in detail in Chapter 5. Laboratory evaluation was done in preparation for field testing and also later as a means to generate comparisons with the equipment.

Prior to the field testing in June 1998, each portable corrosion rate device was used on sample specimens to get practice in the methodology of each particular test routine. SAF permeability tests were performed on various horizontal and vertical surfaces. There appeared to be some correlation between permeability and the corrosion rate measured in the sample specimens.

After the field testing was completed, further tests were conducted with the 3LP device and with the PR-Monitor. These tests were carried out on several beams, shown in Figure 6.2, which underwent continuous wet/dry (two weeks wet and two weeks dry) cycling in a saltwater ponding condition and had previously been examined only with half-cell potential measurements. The Gecor device was not available for this evaluation.

Figure 6.2 The saltwater ponding beams (from an ongoing project at Ferguson Structural Engineering Laboratory) used for corrosion rate testing.

6.2 Corrosion Rate Measurement Equipment

The performance monitoring equipment evaluation includes four corrosion rate devices. Each device uses a form of the polarization resistance method to calculate the corrosion rate of the steel reinforcement.

6.2.1 3LP Device

The 3LP device is a corrosion rate measurement instrument made by

Kenneth C. Clear, Inc. of Virginia. The device was introduced in the1980's as a method for the non-destructive determination of corrosion rate. The ultimate goal of testing with the 3LP device is to quantify corrosion deterioration and predict the remaining life of a structure in service (Kenneth C. Clear 1990). Figure 6.3 shows the layout of the 3LP device, which consists of a self-contained power source and polarization console connected by wire to the electrodes. A sponge serves as the medium for electrode contact.

Figure 6.3 The 3LP device.

The name of the 3LP device is taken from the three-electrode linear polarization setup of the instrument. The setup consists of a reference electrode, a counter electrode, and a working electrode in the same system. Only the

corrosion rate of the working electrode is of interest, and is therefore the only rate measured. The reference electrode is a standard CSE in the form of a pencil electrode for ease in characterizing the corrosion potential (the potential of the working electrode). The counter electrode is a metallic strip, contained in the sponge, used to apply the polarization current. The current is controlled to maintain a constant voltage at the reference electrode. This is a potentiostatic system, where the current is varied to supply the potential in steps. The working electrode is the area of the reinforcing steel being tested. This is calculated as the projection of the steel being polarized beneath the 7.25-in. x 3-in. sponge, which is applied to the concrete surface. Studies have shown that the device may also distribute current to steel in a successive layer of reinforcement, if it is within 6 in. of the probe (Kenneth C. Clear 1990).

The technique for 3LP corrosion rate testing is simple and does not require more than a few minutes. First, the static potential of the test area is recorded from the measurement taken by the reference electrode. Once the static potential is reached without a potential drift, the polarization current is applied until an overpotential of 4mV is reached and the required current is recorded. This is repeated in 4 mV increments to 8mV and 12 mV of overpotential. The device comes with software that calculates the corrosion current density, and therefore the corrosion rate of the reinforcement.

3LP testing may also be performed using permanently embedded probes. Embedded probes are used in areas not easily or conveniently reached with the portable device. The embedded probes consist of a reference and a counter electrode housed inside a section of concrete or grout. The probe is 6-in. long x 3-in. in diameter and requires installation with a minimum of ½ in. of cover. The

counter electrode is 5 in. long inside the probe and polarizes all steel within about 6 in. Measurements are taken with the 3LP console connected to wires running from the probe, which is electrically connected to the working electrode during the installation (Kenneth C. Clear 1990).

6.2.2 The PR-Monitor

The PR-Monitor is a corrosion rate measurement device manufactured by Cortest Instrument Systems, Inc. and supported by Concorr Inc. of Virginia. The PR-Monitor uses the polarization resistance technique to directly determine the corrosion rate of a metal and is specifically designed with reinforced concrete testing in mind.

One attractive feature of the PR-Monitor is that the console is a laptop computer with a specific test program run on the MS-DOS operating system. This allows the operator to assert greater control over the test and to view the actual polarization data as the test is running. The computer also has a relatively large capacity for data storage and performs checks to determine the validity of the data during the test.

In addition to the computer console, the PR-Monitor system includes a 120 volt AC power supply and the reference and counter electrodes with the necessary wiring. The PR-Monitor is displayed in Figure 6.4.

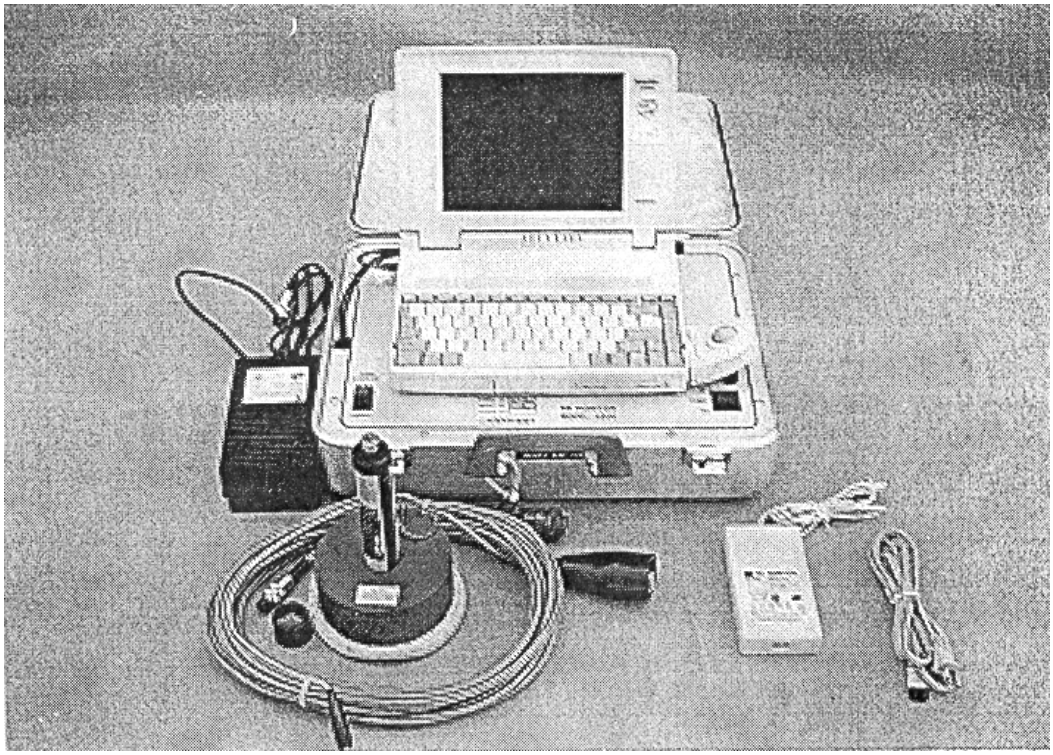

Figure 6.4 The PR-Monitor device (Scannell, Sohanghpurwala, and Islam 1996).

The reference electrode is a standard CSE constructed to fit inside the counter electrode assembly. It is applied to the concrete surface through a sponge prepared in accordance with ASTM C 876-91. The counter electrode is made of platinum and is contained in a guard ring assembly. The guard ring is also platinum. Platinum is an extremely inert metal and will not become active during the testing, allowing for optimum accuracy in measurement (Jones 1996).

The concept of the guard ring is to focus the current output from the counter electrode (CE). This gives a relatively well defined polarized surface and a more accurate measurement of corrosion rate. Figures 6.5 and 6.6 show

schematic diagrams for polarization equipment without and with a guard ring respectively. For comparison, some PR-Monitor measurements were taken with the guard ring deactivated and gave readings much higher than those taken with the guard ring active.

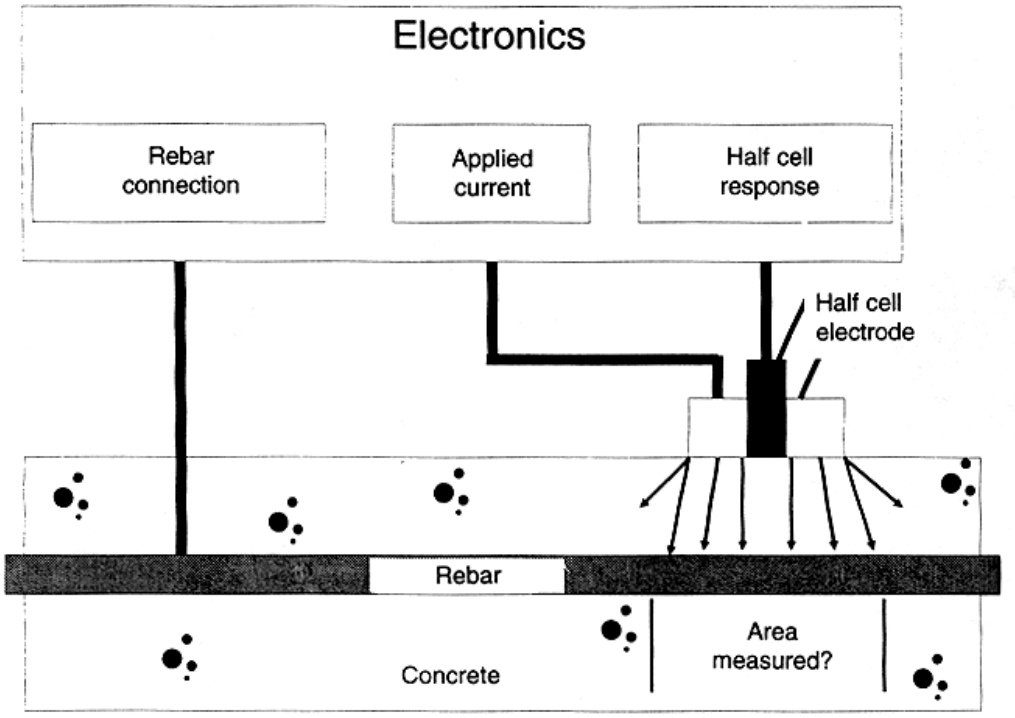

Figure 6.5 Schematic of equipment without a CE guard ring (Broomfield 1997).

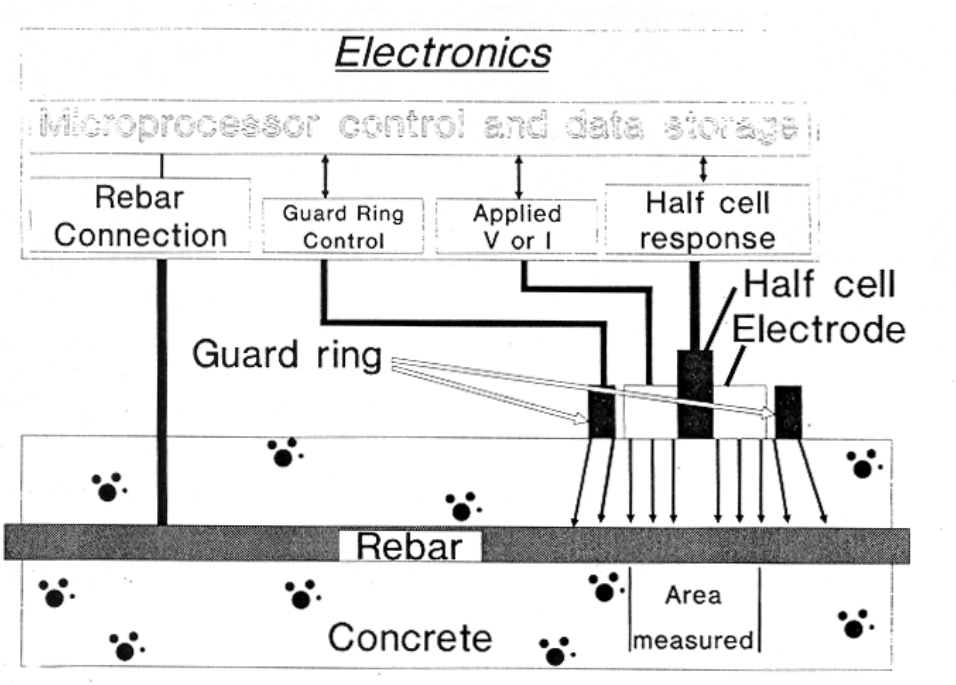

Figure 6.6 Schematic of equipment with a CE guard ring (Broomfield 1997).

The PR-Monitor automatically corrects for the high solution resistance of concrete. The R_s is measured by applying an AC signal to working electrode after the polarization cycle. The value of R_s is then subtacted from the measured polarization resistance to give the equivalent polarization resistance to be used in calculation of the corrosion rate.

Much like the 3LP device, the PR-Monitor uses a polarization based on the application of current to achieve given overpotentials in steps (potentiostatic). The default settings are for step increments of 5mV within the range of –15 mV to +15 mV in comparison with the measured E_{corr}. After the test is completed, the ratio of solution resistance to polarization resistance is calculated. If R_s/R_p is greater than 1.0, the device gives a warning and the operator may re-run the test with the initial overpotential range multiplied approximately by the ratio value.

The overpotential increase is designed to give more accurate data for locations with high solution resistance and may also be input by the operator prior to any test. Such flexibility in operation increases accuracy and decreases the overall test time because a period of 10 minutes is recommended between subsequent tests to avoid effects caused by the previous polarization. The maximum overpotential value is 100 mV (Cortest).

The PR-Monitor outputs a corrosion rate based on the measured value of i_{corr}. The familiar Stern-Geary relationship is applied with an assumed value of the proportioanlity constant set at B = 35 mV. The constant is calculated using values of β_a = 160 mV and β_c = 160 mV; values considered typical for steel in a concrete environment (Cortest).

6.2.2.1 Corrosion Rate Testing with 3LP and PR-Monitor

Additional corrosion rate testing was performed on the beams mentioned in section 6.1.2 with the PR-Monitor and 3LP devices. The beams were separated into four series. There were four beams in the first series, five each in the second series and third series, and two in the fourth series. The first series was composed of reinforced concrete members. The second, third and fourth series of beams all also contained prestressing steel in ducts (West 1999).

Each beam has a unique loading history. Beams 1.4, 2.4, 3.3, 3.4 and 3.5 were all overloaded at least 25 percent above the service load (West 1999). These specimens should have the most severe cracking conditions in their respective series. Beams 1.1 and 3.1 remained unloaded.

Corrosion rate testing was performed at the midspan (location a) and at 12-in. offset from the midspan (location b) on each beam. Table 6.1 shows the results of PR-Monitor testing after 7 months of saltwater exposure. Measurements were also taken with a saturated calomel electrode (the values are adjusted to reflect mV vs. CSE) to test the accuracy of PR-Monitor values.

The results of the testing show that the PR-Monitor generally gave a value of Ecorr lower than the recorded half-cell potential. The difference may be due to the greater depth of penetration achieved with the PR-Monitor; and the consequent measurement of reinforcement in a less corrosive environment. However, the values were relatively accurate; allowing corrosion characterization according to ASTM C 876-91.

The values for corrosion rate correlated with the loading conditions as the beams with higher loading generally show more active corrosion conditions. Many of the higher corrosion rates were observed at locations with some visible cracks. Cracks were visible on beam 1.4, and the corrosion rate could not be determined at either location on this beam. Beams 1.1 and 3.1 have the lowest overall corrosion rates for their respective series, as expected.

Table 6.1 PR-Monitor Values at 7 Months of Exposure.

		Half-Cell	PR-Monitor		
Beam	**Location**	**mV vs CSE**	**Ecorr (mV)**	**Rate (μA/cm^2)**	**Condition**
1.1	a	-147	-122	0.19	Low Rate
	b	-154	-164	0.17	Low
1.2	a	-547	-522	0.64	Moderate
	b	-556	-547	0.85	Moderate
1.3	a	-347	-534	1.01	High
	b	-347	-563	3.50	High
1.4	a	-668	-601	-	N/A
	b	-542	-563	-	N/A
2.1	a	-402	-396	0.46	Low
	b	-522	-507	0.89	Moderate
2.2	a	-592	-593	0.86	Moderate
	b	-585	-580	0.86	Moderate
2.3	a	-561	-546	1.16	High
	b	-515	-510	1.63	High
2.4	a	-497	-487	0.94	Moderate
	b	-572	-565	1.37	High
2.11	a	-547	-541	2.33	High
	b	-557	-555	1.44	High
3.1	a	-187	-164	0.61	Moderate
	b	-202	-187	0.59	Moderate
3.2	a	-208	-207	0.68	Moderate
	b	-233	-234	0.65	Moderate
3.3	a	-405	-374	1.79	High
	b	-271	-256	0.45	Low
3.4	a	-398	-380	1.14	High
	b	-504	-491	3.05	High
3.5	a	-311	-305	1.39	High
	b	-261	-258	1.23	High
4.1	a	-290	-266	2.15	High
	b	-312	-290	1.48	High
4.2	a	-259	-252	3.92	High
	b	-244	-242	3.47	High

Table 6.2 contains the corrosion rate measurement data after 15 months of exposure. Measurements were carried out with both the 3LP device and the PR-Monitor. For the sake of comparison, corrosion rates are shown in μA/cm^2

for both devices and the criterion from each device is used to evaluate the corrosion condition.

Table 6.2 PR-Monitor vs. 3LP for Corrosion Rate Measurement at 15 Months of Exposure.

		3LP Device		PR-Monitor	
Beam	**Location**	**Rate ($\mu A/cm^2$)**	**Condition**	**Rate ($\mu A/cm^2$)**	**Condition**
1.1	a	0.76	Low	0.12	Low
	b	1.15	Moderate	0.19	Low
1.2	a	4.37	Moderate	0.88	Moderate
	b	5.79	Moderate	1.17	High
1.3	a	3.50	Moderate	1.06	High
	b	6.29	Moderate	1.30	High
1.4	a	5.64	Moderate	1.76	High
	b	7.66	Moderate	2.75	High
2.1	a	5.58	Moderate	0.85	Moderate
	b	9.32	High	2.59	High
2.2	a	5.61	Moderate	0.95	Moderate
	b	4.86	Moderate	0.91	Moderate
2.3	a	6.33	Moderate	0.47	Moderate
	b	4.79	Moderate	1.42	High
2.4	a	4.25	Moderate	0.87	Moderate
	b	6.78	Moderate	1.94	High
2.11	a	6.70	Moderate	1.27	High
	b	7.08	Moderate	2.19	High
3.1	a	4.44	Moderate	0.14	Low
	b	4.62	Moderate	0.31	Low
3.2	a	5.43	Moderate	0.32	Low
	b	6.83	Moderate	0.42	Low
3.3	a	14.14	High	1.22	High
	b	6.56	Moderate	0.45	Low
3.4	a	14.53	High	1.12	High
	b	25.14	High	2.48	High
3.5	a	17.41	High	1.24	High
	b	13.32	High	1.20	High
4.1	a	8.88	Moderate	0.87	Moderate
	b	12.28	High	1.02	High
4.2	a	7.16	Moderate	0.69	Moderate
	b	8.75	Moderate	0.79	Moderate

The corrosion rate values given by the 3LP device were much higher than those from the PR-Monitor. The area used in the corrosion rate calculation may be smaller than the actual polarized area of steel due to a lack of current confinement (West 1999). The polarization current from the PR-Monitor is confined by the guard ring. In spite of the higher rates from the 3LP device, the corrosion rate guidelines from each instrument actually indicate that more severe conditions can be diagnosed with the PR-Monitor.

There was correlation between the corrosion rate trends of the 3LP and the PR-Monitor devices. All of the locations where the 3LP device indicated a "High" corrosion condition, the PR-Monitor also characterized the rate as "High". The 3LP seems to have a larger range for "Moderate" corrosion conditions. It should be noted that comparisons between these two devices are not absolute because they are of different size and shape, and therefore measure different areas of reinforcement. Both devices showed lower corrosion rates in the unloaded specimens.

The discrepancy between the values from the 3LP and PR-Monitor suggests that the corrosion evaluation should not be made on a quantitative basis, but rather should be a qualitative analysis based on the guidelines provided for each device. However, it is likely that the values given by the PR-Monitor were closer to the actual reinforcement corrosion rates.

6.2.3 Gecor Device

The Gecor 6 Corrosion Rate Meter is for use on steel in concrete and is

manufactured by James Instruments, Inc. This device uses the polarization resistance method for measurement of corrosion rate. The value used for the proportionality constant is 26 mV. Gecor 6 is shown in Figure 6.7.

Figure 6.7 Gecor 6 device – sensors and rate meter (James Instruments).

Gecor 6 uses the guard-ring concept to confine the current distribution. The device has two stainless steel counter electrodes, one central and one external on the corrosion rate sensor (Sensor A), seen in Figure 6.8.

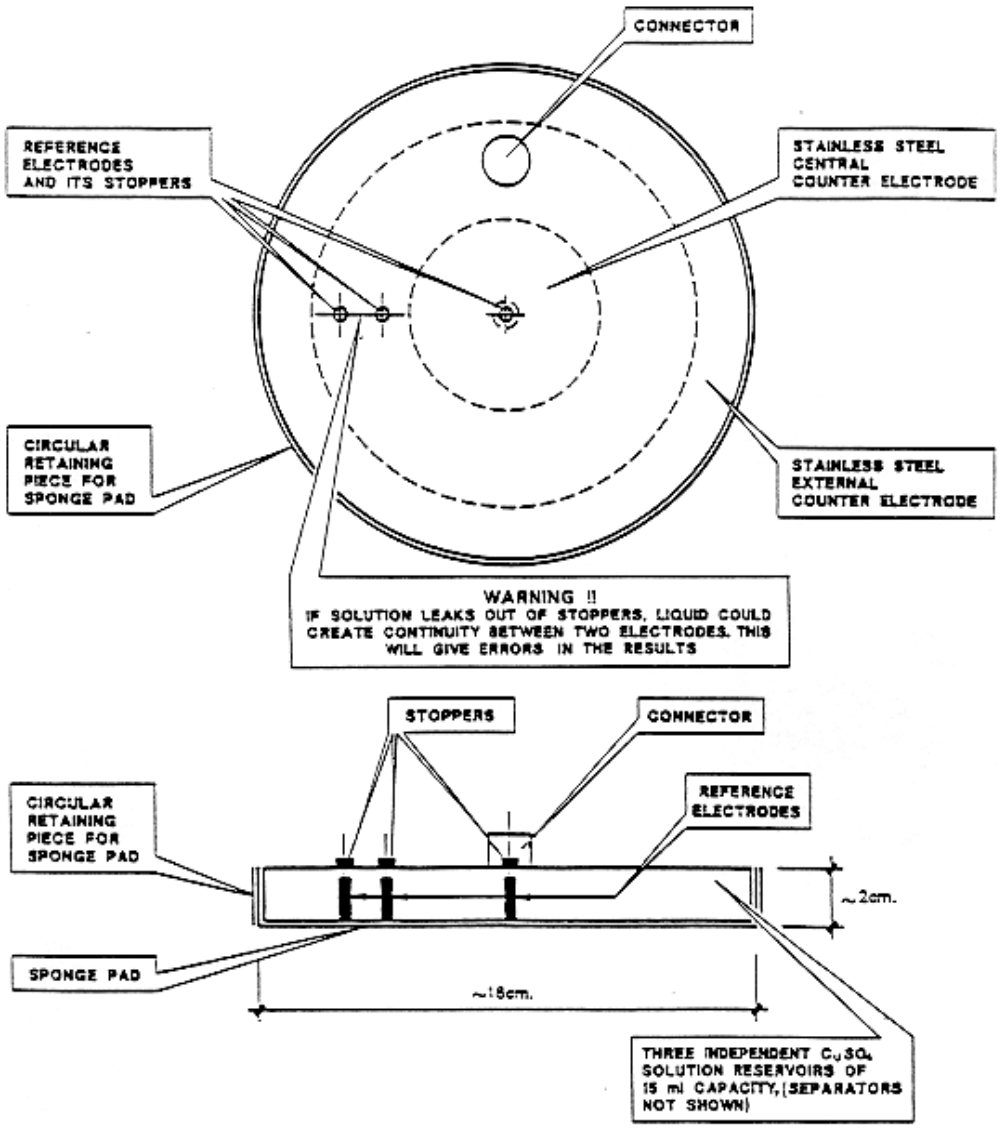

Figure 6.8 Schematic of the corrosion rate sensor for Gecor 6 (James Instruments).

There are three $Cu/CuSO_4$ reference electrodes - a central electrode and two confinement electrodes. For operation, each electrode has a reservoir of $CuSO_4$ solution. Some refilling is required prior to testing, especially after

storage of the device, due to solution leakage from the reference electrodes. Any entrapped air must be removed from the reservoirs during the refilling process. The electrode sensors must be cleaned before each test to remove crystals and to prevent continuity between the electrodes during data collection. A sponge is provided for use between the Gecor 6 and the concrete surface. When wetted, the sponge supplies an electrical connection to the surface and helps correct for any surface irregularities (James Instruments).

For corrosion rate measurement, the Gecor 6 device should be centered over a reinforcing bar or over a junction of two bars with known diameters. The steel surface being tested is simply the bar surface area covered by the 10.5 cm. sensor. An electrical connection to the working electrode is required. The corrosion rate sensor, which contains the reference electrodes and the counter electrode, is connected to the Rate Meter by a connection cable. The cable also includes the ground connection to the working electrode. The Rate Meter is a battery-operated console. Once the area of steel is provided as input to the Rate Meter, the test can begin. The Gecor 6 device determines Ecorr and checks for potential drift. When the operator elects to proceed, the current is applied and polarization begins. In addition to Ecorr, the Gecor 6 device measures the corrosion rate and the concrete resistivity.

6.2.4 Concorr Embedded Corrosion Rate Probe

The portable field test devices were extremely useful and convenient, however in some applications it may be preferable to have a permanent, non-destructive testing procedure. Embedded probes are designed to be cast into the concrete or repair material matrix to allow repeated testing at probe locations

without the difficulties associated with portable testing equipment. Embedded probes also include a ground wire to the working electrode. Wires from the counter electrode, reference electrode, and working electrode may be combined in a cable extending out of the concrete member for ease of measurement.

Embedded probes were considered to be desirable devices for use in Project CSR 783-2-66 because it is important to avoid penetration of the Fibrwrap® system. The probes used for this study are manufactured by Concorr, Inc. of Virginia. A schematic diagram of the probes is shown in Figure 6.9.

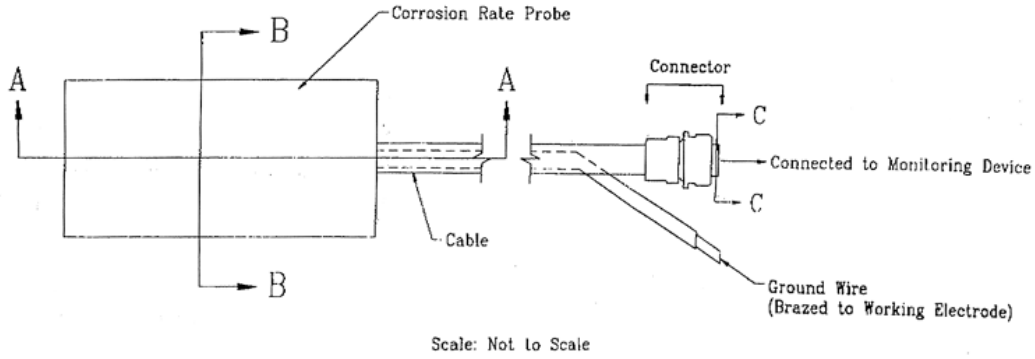

Figure 6.9 Concorr corrosion rate probe and connection cable (Concorr, 1998).

The electrodes are encased in a mortar block. The outer dimensions of the probes are 2 3/8-in. x 2 3/8-in. x 5-in. The mortar block protects the electrodes and houses them in a consistent cementitious environment. Figures 6.10 and 6.11 show the sections of the probes. Figure 6.10 is a lengthwise view showing electrode placement and the wiring diagram inside the mortar block.

The ground wire is routed into the connection cable along with the wires from the reference and counter electrodes for access to the measurement device.

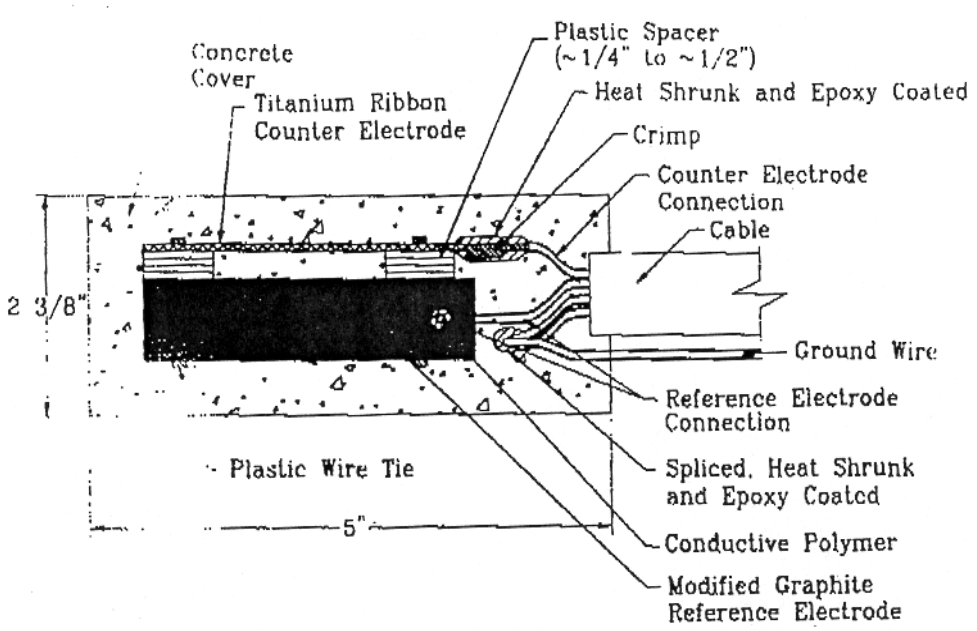

Figure 6.10 Lengthwise section of embedded corrosion rate probe.

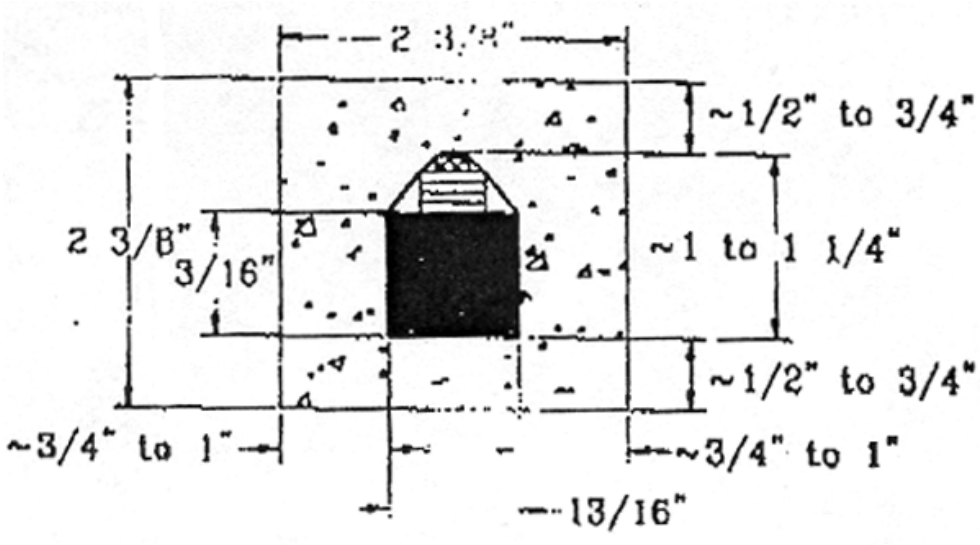

Figure 6.11 Cross-section of embedded corrosion rate probe.

The reference electrode is modified graphite, an extremely inert material. The counter electrode is a titanium ribbon and is mounted on top of the reference electrode inside the probe. During installation it is preferable to locate the reinforcement in the path of the current from the counter electrode. However, the graphite reference electrode should not be placed between the counter electrode and the steel. The test area, or the area of polarized steel, is calculated based on the installation. The test area is confined to the length of the probe, with little current "spread" beyond this region. Only reinforcement in close proximity to the probe is affected by the polarization. The connector on the end of the connection cable, displayed in Figure 6.9, is a six-pin connector designed for input to the PR-Monitor corrosion rate device.

Other embedded testing devices include the 3LP embedded probe, mentioned in section 6.2.1, and some permanent reference electrodes manufactured by Electrochemical Devices, Inc. (EDI). EDI has two electrode models: Model IT and Model CB. Model IT is a reference electrode composed of a gel, either Ag-AgCl or Cu-$CuSO_4$, in a PVC housing and is used to measure the potential of the reinforcement. Model CB consists of a AG-AgCl electrode with a wire running to the reinforcement and a cable for external access. The electrode is surrounded by a backfill material compatible with the concrete environment to provide consistent continuity.

6.3 Surface Air Flow (SAF) Permeability Device

The SAF device allows for field testing of concrete relative permeability.

The device applies a vacuum of about 125 mm Hg, measuring the flow of air to a depth of ½ in. into the concrete. The system is operated from a rechargeable battery, which powers a small motorized pump to generate the vacuum over a small plate (vacuum plate). The pump and battery are kept in a back-pack, making the SAF device portable and permitting rapid testing at different locations.

During operation, the vacuum plate is applied to the concrete surface. The plate is sealed with a circumferential foam pad, which compresses between the plate and the surface, confining the vacuum. The plate is detachable for use on vertical and overhead surfaces, further extending the portable capabilities of the SAF device.

The SAF test procedure calls for a calibration at a vacuum of 750 to 765 mm Hg as mentioned in section 5.1.4. The particular equipment used in this study could not reach this value and therefore the flow rate values may have been artificially high. In fact, the values determined on the structure on Project CSR 783-2-66 indicated very high flow rates at all locations (see Table 5.4). The results of the ASTM permeability test were more reasonable and consistant in this study.

The SAF device was very quick and efficient to use, but the results cannot be used quantitatively for a condition evaluation. For the best results, tests should be conducted many times on a given structural element and compared to the results of a standard test – such as the ASTM permeability test. In addition, SAF testing is adversely affected where surface cracks are present.

Cracks limit the effectiveness of the device on structures with delamination and spalling from existing corrosion.

Chapter 7

SUMMARY AND CONCLUSIONS

7.1 Summary

Effective repair methods have become important to address a major problem related to our infrastructure, corrosion-related deterioration of reinforced concrete structures. FRP composite wrapping has been used to prevent seismic overloading; but to evaluate the performance of FRP wrapping systems in corrosive environments, laboratory and field research programs are needed. Corrosion-damaged bridge overpass structures are being monitored after they have been repaired and wrapped with an FRP system. The effectiveness of several performance monitoring instruments for use in the field was evaluated. The equipment included portable devices for field testing and permanent instrumentation for in-service testing of corrosion activity.

7.2 FRP Composite Wrapping Systems for Corrosion Protection

The performance of FRP wrapping systems used for corrosion repairs and for prevention against further corrosion in previously exposed areas has not been encouraging. The corrosion rate data collected from the wrapped structures in Project CSR 783-2-66 will provide valuable information on in-service performance. Similarly, the corrosion behavior of wrapped laboratory specimens with chlorides inherent in the concrete mix design is also being monitored (Fuentes 1999). The monitoring of laboratory specimens without mix chlorides

can be used to assess the corrosion performance of wrapping systems on uncontaminated and uncorroded structures.

The application of wrapping systems in both the laboratory and in the field was a convenient process. FRP wrapping is easy to place and can be applied quickly.

7.3 Performance Monitoring Equipment

The use of performance monitoring equipment is essential in understanding the corrosion process in deteriorating structures. Portable devices are especially useful and allow for extensive and repeatable testing. It is important that the equipment is well-maintained and working properly.

The corrosion rate devices used in this study all operate with the polarization resistance method. Portable testing was done with the 3LP device, PR-Monitor device, and the Gecor device. Embedded electrodes are in place for continued in-service evaluation. The following observations are based on the research involving the equipment.

- The 3LP and PR-Monitor device showed consistent corrosion rate trends.
- Corrosion rate values from field testing are qualitative, but not quantitative.
- The PR-Monitor was the best device for field corrosion rate testing.
- Embedded corrosion rate probes were convenient for in-service testing.
- Chloride contents from damaged areas of the structures in Project CSR 783-2-66 were above the threshold for probable corrosion.

- Chloride content measurements correlated with corrosion rate measurements and with visible delamination and spalling.
- Chloride profiles indicated high concrete permeability on Project CSR 783-2-66, in agreement with standard permeability tests.
- The SAF permeability device gave inconsistent results and showed only loose correlation with standard permeability testing.

7.4 Recommendations for Continuing and Further Research

This report details and summarizes the beginning phases of a long-term corrosion study. The most important aspect of this research is that it is continued until definite conclusions on the effect of FRP wrapping systems on corrosion behavior are reached. It is recommended that in-service corrosion rate measurements be taken indefinitely at six-month intervals, with regular evaluation of the values. It is further recommended that the laboratory research continue for 4 to 5 years, concluding with autopsies of each specimen.

Further research of fiber-reinforced composite wrapping systems is needed. Areas of possible research include corrosion protection offered under different loading conditions, detailed analysis of capillary action in submerged elements with partial wrapping, and the development of new wrap systems.

Future research relating to performance monitoring equipment is also important. The development of better equipment and more comprehensive monitoring programs would make structural repair and maintenance more effective and could become an important step toward infrastructure

improvement. Research involving the application of various non-destructive test methods would be particularly useful.

Appendix A

TYFO® S FIBRWRAP® MATERIAL PROPERTIES*

Composite Material Properties	SEH 51/Tyfo® S Epoxy (Primary Glass Fabric)	SCH 41S/Tyfo® S Epoxy (Primary Carbon Fiber)
Ultimate Tension Strength	80 ksi (552 MPa)	150 ksi (1,034 MPa)
Ultimate Elongation	2.0 %	1.5 %
Elastic Modulus	4,000 ksi (27,579 MPa)	10,000 ksi (68,948 MPa)
Design Thickness	0.051 in. (1.3 mm) per layer	0.041 in. (1.0 mm) per layer

*Reproduced from Delta Structural Technologies, Inc.

Appendix B

PRODUCTS USED ON PROJECT CSR 783-2-66**

B.1 Repair Material

SHOTPATCH 21F

Silica fume enhanced, fiber reinforced structural shotcrete for wet or dry process applications

DESCRIPTION:

SHOTPATCH® 21F is a pre-packaged silica fume enhanced, fiber reinforced mortar which contains an integral corrosion inhibitor. The unique technology of SHOTPATCH 21F allows for application by either the wet or dry shotcrete process. The result is a high quality structural repair material which exhibits high bond strengths, low permeability and excellent resistance to freeze-thaw cycling and salt scaling.

Application Thickness:

- Minimum application thickness is 3/8" in. (10 mm)
- Recommended maximum application thickness per lift is 6 in. (152 mm). Deeper applications are possible depending on the size and configuration of the repair.

RECOMMENDED FOR:

Structural repair and retrofit of:

- Dridges, tunnels, and parking garages
- Piers, docks and dams
- Reservoirs and tanks
- Treatment facilities
- Canals and aqueducts

FEATURES/BENEFITS:

- Fiber reinforced - for plastic shrinkage control and reduced rebound
- Versatile - designed for use with the dry or wet shotcrete process
- Low permeability - resists water and chloride ion penetration
- Corrosion resistant - contains an integral corrosion inhibitor
- Workable - easy to cut and finish
- Pre-packaged quality - bag-to-bag uniformity

STANDARDS COMPLIANCE:

Sand gradation meets ASTM C 33 and ACI 506 standards. Cement meets ASTM C 150, Type II requirements.

PACKAGING/ESTIMATING:

SHOTPATCH 21F is supplied in 55 lb (25 kg) moisture-resistant bags which yield approximately 0.48 ft³ (0.013 m³). This will cover approximately 5.8 ft² (0.54 m²) at a 1 in. (25 mm) depth before rebound and waste. The product is also available in 3,300 lb (1,497 kg) bulk bags.

PERFORMANCE DATA:

Results were obtained when material was mixed with 0.8 gal (3.0 L) of water per bag and cured at 73 °F (22 °C). Reasonable variations can be expected depending upon application methods, test methods, and curing conditions.

PLASTIC PROPERTIES:

Unit Weight	129 lb/ft³ (2,067 kg/m³)

Set Times, (hr:min) *(ASTM C 266)*	**Initial Set**	**Final Set**
	2:45	6:00

HARDENED PROPERTIES:	**1 Day psi (MPa)**	**7 Day psi (MPa)**	**28 Day psi (MPa)**
Direct Tensile Bond Strength *(ACI 503R, Appendix A)*	50 (0.3)	130 (0.9)	180 (1.2)
Slant Shear Bond Strength *(ASTM C 882 Modified[2])*	1200 (8.3)	2500 (17.2)	3000 (20.7)
Drying Shrinkage at 28 Days *(ASTM C 157 Modified[2])*			0.06%
Modulus of Elasticity at 28 Days *(ASTM C 469)*			4.6 x 10⁶ psi (31.7 GPa)
Rapid Chloride Permeability at 28 Days *(ASTM C 1202/AASHTO T 277)*			685 coulombs
Freeze-Thaw Resistance at 300 Cycles *(ASTM C 666 Procedure A)*			95% RDM

Abrasion Resistance *(ASTM C 779)*	**Duration**	**Depth of Wear**
	30 Minutes	0.021 in. (0.53 mm)
	60 Minutes	0.036 in. (0.91 mm)

	1 Day psi (MPa)	**7 Day psi (MPa)**	**28 Day psi (MPa)**
Splitting Tensile Strength *(ASTM C 496)*	200 (1.4)	300 (2.1)	400 (2.8)
Flexural Strength *(ASTM C 348)*	600 (4.1)	1200 (8.3)	1800 (12.4)
Compressive Strength *(ASTM C 109)*	2500 (17.2)	6000 (41.4)	7000 (48.3)

	3 Day psi (MPa)	**28 day psi (MPa)**
Compressive Strength *(ASTM C 42)*		
Dry Process	6,000 (41.4)	10,000 (69.0)
Wet Process	6,000 (41.4)	10,000 (69.0)

[1] No epoxy bonding agent used
[2] ICRI Guideline #03733, 1" x 1" x 10" prism

**Reproduced from Manufacturers' Product Data Sheets

SURFACE PREPARATION:

Concrete: Perform surface preparation in compliance with ICRI Technical Guideline No. 03730 "Guideline for Surface Preparation for the Repair of Deteriorated Concrete Resulting from Reinforcing Steel Corrosion" and ACI 506.2 "Specification for Materials, Proportioning, and Application of Shotcrete". Remove all unsound or delaminated concrete providing a minimum 1/4 in. (6 mm) substrate profile amplitude and 3/4 in. (19 mm) clearance behind corroded reinforcing steel. The perimeter of the area to be patched should be tapered toward the center at approximately 45° to prevent square and feather edges, or saw cut to a minimum depth 1/4 in. (6 mm). After concrete removal and prior to placement, mechanically abrade the concrete surface to remove all bond-inhibiting materials from the concrete substrate and to provide additional mechanical bond. Presoak the prepared concrete surface to provide a saturated, surface dry (SSD) condition.

Corroded reinforcing steel: Remove all oxidation and scale from the exposed reinforcing steel in accordance with ICRI Technical Guideline No. 03730 "Guideline for Surface Preparation for the Repair of Deteriorated Concrete Resulting from Reinforcing Steel Corrosion". For additional protection from future corrosion, coat the prepared reinforcing steel with EMACO® P-22 or P-24 rebar coatings.

MIXING:

Wet process: Add 0.7 to 0.9 gal (2.7 to 3.4 L) of potable water per 55 lb (25 kg) bag of SHOTPATCH 21F. Mechanically mix using an appropriate size mortar mixer. Pour approximately 90% of the water into the mixing container then charge the mixer with the bagged material. Add the remaining mix water as required. Mix for 3 to 5 minutes until a homogenous consistency is achieved.

APPLICATION:

The installation of Shotpatch 21F is dependent primarily upon the skill of the nozzleman. Apply SHOTPATCH 21F in accordance with ACI 506R "Guide to Shotcrete". Remove excess water from the saturated substrate and apply while taking proper consideration for rebound and compaction around reinforcing steel. When applying with multiple lifts, scratch the preliminary lift before initial set. Apply the succeeding lift after the preliminary lift has reached final set. If the succeeding lift is not to be immediately placed, keep the surface continually moist. Cut-off or level as required matching the original concrete elevation. Where rapid drying conditions exist (such as hot, dry, and windy conditions) use CONFILM® evaporation reducer. Finish the final surface as required.

CURING:

Proper curing is extremely important and should be conducted in accordance with ACI 308 "Standard Practice for Curing Concrete". Apply a curing compound which complies with the moisture retention requirements of ASTM C 309 such as MASTERCURE® 100W or 200W or moist cure for a minimum of 7 days.

SAFETY:

For industrial and professional use only. Refer to MSDS before use. Wear appropriate protective clothing and eye protection.

LIMITATIONS:

Minimum application thickness is 3/8 in. (10 mm). Do not mix partial bags. Minimum ambient and surface temperatures should be 45 °F (7 °C) and rising at the time of application.

STORAGE AND SHELF LIFE:

Unopened bags have a shelf life of 12 months when stored under cover in dry conditions between 45 °F (7 °C) and 90 °F (32 °C).

RELATED BULLETINS:

Material Safety Data Sheet - SHOTPATCH 21F
Specification Bulletin

B.2 Corrosion Inhibitor

Macropoxy 920 Pre-Prime (B58T101)

Description

Macropoxy 920 Pre-Prime is a 100% solids, VOC compliant, rust penetrating epoxy pre-primer designed for use over marginally prepared surfaces when a thorough cleaning is not possible.

- A penetrating sealer for tight rusted surfaces
- High solids (100%)
- Multi-surface coating
- Low viscosity
- Low VOC

Part A	B58T101	Transparent
Part B	B58V10	Hardener

Characteristics

Finish:			Medium Sheen
Color:			Transparent
Volume Solids (calculated):			100%, mixed 74%, ASTM D2697
VOC (EPA Method 24):			138 g/L; 1.15 lb/gal, mixed
Mix Ratio:			2 components, 3:1 mix by volume
Recommended Spreading Rate per coat:			
Wet mils:			1.5 - 2.0
Dry mils:			1.5 - 2.0
Coverage:			800 - 1,050 sq ft/gal approximate
Drying Schedule @ 2.0 mils wet @ 50% RH:			
	@ 40°F	**@ 77°F**	**@ 120°F**
To touch:	18 hours	9½ hours	7 hours
Tack-free:	32 hours	17 hours	14 hours
To recoat:	36 hours	overnight	overnight
Pot Life:	8-10 hours	4 hours	3-4 hours

Drying time is temperature, humidity, and film thickness dependent.

Sweat-in-time: none required

Flash Point: 152°F, PMCC, mixed

Application

See Note 2, 4, & 5, page 152

Temperature: 40°F minimum, 100°F maximum (air, surface, and material), at least 5°F above dew point
Relative humidity: 85% maximum

The following is a guide. Changes in pressures and tip sizes may be needed for proper spray characteristics. Always purge spray equipment before use with listed reducer. Any reduction must be compatible with the existing environmental and application conditions.

Reducer/Clean-Up ..... Reducer #54, R7K54 clean up only

Airless Spray ..... Not recommended

Conventional Spray

Gun	Binks 95
Tip	66
Cap	63 PB
Atomization Pressure	50 psi
Fluid Pressure	10 psi

Brush ..... Natural Bristle

Roller ..... 1/4"-3/8" woven with phenolic core

Specifications

Steel:
1 ct. Macropoxy 920 Pre-Prime @ 1.5 - 2.0 mils dft
1 ct. Macropoxy Primer @ 3.0 - 6.0 mils dft
1 ct. Macropoxy HS @ 3.0 - 6.0 mils dft

Steel, zinc-rich primer:
1 ct. Zinc Clad IV @ 3.0 - 5.0 mils dft
1 ct. Macropoxy 920 Pre-Prime @ 1.5 - 2.0 mils dft
1 ct. Heavy Duty Epoxy @ 5.0 - 7.0 mils dft
1 ct. Hi-Solids Polyurethane @ 3.0 - 4.0 mils dft

Masonry:
1 ct. Macropoxy 920 Pre-Prime @ 1.5 - 2.0 mils dft
1-2 cts. Tile-Clad Hi-Solids @ 2.5 - 4.0 mils dft

Performance Specifications

- Designed for industrial and marine environments
- Penetrates existing, tightly adhered rust to provide a "tight" substrate prior to subsequent coats
- Can also be used as a high performance primer/sealer for masonry surfaces
- Not for immersion service
- Dry heat resistance up to 200°F

Epoxy coatings may darken or yellow following application and curing.

Appendix C

CORROSION RATE DATA SHEETS

Corrosion Rate Measurement Data Sheet

Project 1774 Sheet ___1__

Date	6-30-98
Bridge Location (Lubbock, TX)	6282/289/EB
Bridge ID #	Structure #8
Sample ID #	6282/289/EB1
Sample Location: 10 feet from downstream end, to the left of the column on the East face.	**Comments:** ➢ Use exposed steel from coring for the electrical connection.

Polarization Data:

3LP Data:
Static Voltage: 40mV Cu-$CuSO_4$

Voltage (mv)	Current (mA)
0	007
4	18
8	33
12	47

Gecor Data:

Icorr = 0.01μA/cm^2
Ecorr = 83.8 mV
Rp = 29.75 ko

File: 62822895

PRMonitor:

Ecorr = 108 mV
Icorr = 0.219μA/cm^2
Rate = 0.01mpy

Concrete Surface Description:

- ➢ Sealant on the surface.
- ➢ Wipe off dirt and bird feces.
- ➢ No visible cracks at sample location.

Half-Cell Potential (mV vs. Cu-$CuSO_4$)	915
PR Monitor Filename	62822895

Corrosion Rate Measurement Data Sheet

Project 1774 Sheet __2___

Date	6-30-98
Bridge Location (Lubbock, TX)	6282/289/WB
Bridge ID #	Structure #7
Sample ID #	6282/289/WB1
Sample Location: 1st bent on the west face, about 20 feet from downstream end.	**Comments:** ➢ Crack runs through ground area on concrete surface. ➢ As = 25.92 in^2 ➢ Too sensitive for 3LP

Polarization Data:

3LP Data:
Static Voltage: N/A

Voltage (mv)	Current (mA)
N/A	N/A

Gecor Data:
Icorr = N/A
Ecorr = N/A
Rp = N/A

PRMonitor:
Ecorr = N/A
Rate = N/A

File: 622891

Concrete Surface Description:

Half-Cell Potential (mV vs. Cu-$CuSO_4$)	54
PR Monitor Filename	622891a

Corrosion Rate Measurement Data Sheet

Project 1774 Sheet __3___

Date	6-30-98
Bridge Location (Lubbock, TX)	6282/289/WB
Bridge ID #	Structure #7
Sample ID #	6282/289/WB1
Sample Location: 1st bent, on west face – about 12 feet from downstream end.	**Comments:** ➢ Close to top, over stirrup. ➢ As = 11.775 in^2 ➢ As = 115 cm^2 for #11 bar.

Polarization Data:

3LP Data:		**Gecor Data:**	**PRMonitor:**
Static Voltage: N/A			
		Icorr = 0.001μA/cm^2	Ecorr = 79.2 mV
Voltage (mv)	Current (mA)	Ecorr = 78.3 mV	Icorr = 0.46 μA/cm^2
N/A	N/A	Rp = 21.64 ko	Rate = 0.21 mpy
		File: 622892	

Concrete Surface Description:

Half-Cell Potential (mV vs. Cu-$CuSO_4$)	70
PR Monitor Filename	622891b

Corrosion Rate Measurement Data Sheet Project 1774 Sheet ___4__	
Date	7-1-98
Bridge Location (Lubbock, TX)	Route 289 EB at Municipal Drive – 289/MD/EB
Bridge ID #	Structure #2
Sample ID #	289/MD/EB6/Center
Sample Location: Immediately left of interior column.	**Comments:** ➢ Reinforcement may have not been continuous. ➢ No readings.
Polarization Data: No Data Collected.	
Concrete Surface Description: ➢ Cracking at the bottom of bent. ➢ Paint and epoxy repair on surface make grinding difficult and may improve resistance values.	
Half-Cell Potential (mV vs. Cu-$CuSO_4$)	None.
PR Monitor Filename	289MD6b

Corrosion Rate Measurement Data Sheet Project 1774 Sheet ___5__	
Date	7-1-98
Bridge Location (Lubbock, TX)	289/MD/EB
Bridge ID #	Structure #2
Sample ID #	289/MD/EB6/17
Sample Location: About 17 feet from the downstream end.	**Comments:** ➢ Delaminations cause bad data. ➢ PR-Monitor and Gecor devices did not give good data.
Polarization Data: None.	
Concrete Surface Description: ➢ Delaminated and spalling concrete.	
Half-Cell Potential (mV vs. Cu-$CuSO_4$)	1370
PR Monitor Filename	289md6a

Corrosion Rate Measurement Data Sheet

Project 1774 Sheet ___6___

Date	7-1-98
Bridge Location (Lubbock, TX)	289/MD/WB
Bridge ID #	Structure #1
Sample ID #	289/MD/WB2/End
Sample Location: On the downstream end.	**Comments:** ➢ Used hammer to check for delaminations and to expose steel. ➢ The Gecor readings were difficult to stabilize.

Polarization Data:

3LP Data:
Static Voltage: 100mV Cu-$CuSO_4$

Voltage (mv)	Current (mA)
0	12
4	21
8	32
12	40

Gecor Data:
Icorr = 0.009μA/cm^2
Ecorr = 116.4 mV
Rp = 13.48 ko

File: 2899992

PRMonitor:
Ecorr = 108 mV
Icorr = 0.0044μA/cm^2
Rate = 0.002 mpy

Concrete Surface Description:

➢ Delamination on top surface of bent.

Half-Cell Potential (mV vs. Cu-$CuSO_4$)	
PR Monitor Filename	289MDW2

Corrosion Rate Measurement Data Sheet

Project 1774 Sheet ___7__

Date	7-1-98
Bridge Location (Lubbock, TX)	6282 and Mainlane Overpass Interchange (Westbound traffic) – 6282/WB
Bridge ID #	Structure #5
Sample ID #	6282/MO/WB
Sample Location: Between the 3rd and 4th column from downstream end.	**Comments:** ➢ Cracks and rust-stains on the concrete surface. ➢ Difficult to establish connection with steel.

Polarization Data:

3LP Data:
Static Voltage: 270mV Cu-$CuSO_4$

Voltage (mv)	Current (mA)
0	26
4	42
8	55
12	68

Gecor Data:
Icorr = 0.003μA/cm^2
Ecorr = 41.4 mV
Rp = 17.39 ko

File: 628201

PRMonitor:
Ecorr = 74.9 mV
Icorr = 0.018μA/cm^2
Rate = 0.008 mpy

Concrete Surface Description:

➢ Significant cracking.

Half-Cell Potential (mV vs. Cu-$CuSO_4$)	None.
PR Monitor Filename	6282IW5

Corrosion Rate Measurement Data Sheet Project 1774 Sheet ___8__	
Date	7-2-98
Bridge Location (Lubbock, TX)	US 84 and FM 41 Eastbound – 84/41/EB
Bridge ID #	Structure #10
Sample ID #	84/41/EB/1
Sample Location: Between center and right column on the East face of the bent.	**Comments:** ➢ Thick paint/coating layer – grinding is difficult. ➢ Some repair patches. ➢ Could not stabilize 3LP.
Polarization Data: **3LP Data:** None.	**Gecor Data:** Icorr = 0.008μA/cm^2 Ecorr = 49.8 mV Rp = 14.05 ko Filename: 84411
	PRMonitor: Ecorr = 66.8 mV Icorr = 0.15 μA/cm^2 Rate = 0.069 mpy
Concrete Surface Description:	
Half-Cell Potential (mV vs. Cu-$CuSO_4$)	55
PR Monitor Filename	8441EB1

Corrosion Rate Measurement Data Sheet

Project 1774 Sheet ___9__

Date	7-2-98
Bridge Location (Lubbock, TX)	84 and FM 400 (2nd bent in Eastbound direction) – 84/400/EB
Bridge ID #	Structure #11
Sample ID #	84/400/EB2
Sample Location: On the top of the bent.	**Comments:** ➢ Severe delamination and spalling at the bottom of column – steel exposed. ➢ Cracks in concrete and paint peeling off at the bottom of the bent.

Polarization Data:

3LP Data:

Static Voltage: 157mV Cu-$CuSO_4$

Voltage (mv)	Current (mA)
0	0
4	203
8	309
12	421

Gecor Data:

Icorr = 0.022μA/cm^2
Ecorr = 113 mV
Rp = 1.59 ko

File: 844002

PRMonitor:

Ecorr = 144.5 mV
Icorr = 0.302μA/cm^2
Rate = 0.138 mpy

Concrete Surface Description:

Half-Cell Potential (mV vs. Cu-$CuSO_4$)	
PR Monitor Filename	84400E2

Appendix D

CHLORIDE SAMPLE DATA SHEETS

Chloride Sample Data Sheet Project 1774 Sheet __1____	
Date	6-30-98
Weather Condition	Sunny – clear sky
Bridge Location	6282/289/EB (5^{th} bent in direction of EB traffic on 62/82)
Bridge ID #	Structure #8
Sample ID #	6282/289/EB5/10/1 6282/289/EB5/10/1.5 6282/289/EB5/10/2
Sample Location: 10 feet in from downstream end	**Comments:** ➢ Drill to ½" – disregard dust. Start Collecting at ½" to eliminate surface irregularities. ➢ Drill 3 holes – mix dust to get enough for various tests: each bag is an average from 3 locations.
Concrete Surface Description:	

Chloride Sample Data Sheet Project 1774 Sheet ___2___	
Date	6-30-98
Weather Condition	Sunny – clear
Bridge Location	6282/289/EB
Bridge ID #	Structure #8
Sample ID #	6282/298/EB5/2.5/1 6282/298/EB5/2.5/1.5 6282/298/EB5/2.5/2
Sample Location: 2.5 feet from downstream end.	**Comments:** ➢ Concrete pieces fall off easily – severe corrosion (corrosion stains, spalling).
Concrete Surface Description: ➢ Paint is falling off- many cracks, corrosion stains.	

Chloride Sample Data Sheet Project 1774 Sheet ___3___	
Date	6-30-98
Weather Condition	Sunny – clear
Bridge Location	6282/289/WB
Bridge ID #	Structure #7
Sample ID #	6282/289/WB1/20/1 6282/289/WB1/20/1.5 6282/289/WB1/20/2
Sample Location: About 20 feet from the downstream end.	**Comments:** ➢ 3 holes at each depth.
Concrete Surface Description: ➢ Dirty- some cracks. ➢ Water stains in this area.	

Chloride Sample Data Sheet Project 1774 Sheet ___4___	
Date	6-30-98
Weather Condition	Windy – increasingly cloudy
Bridge Location	6282/289/WB
Bridge ID #	Structure #7
Sample ID #	6282/289/WB1/12/1 6282/289/WB1/12/1.5 6282/289/WB1/12/2
Sample Location: About 12 feet from the downstream end.	**Comments:** ➢ Drilled 4 holes, but disregard the dust from one due to an air pocket.
Concrete Surface Description:	

Chloride Sample Data Sheet Project 1774 Sheet ___5___	
Date	7-1-98
Weather Condition	Clear and calm, 85 degrees
Bridge Location	289/6282/SB: West column on 3rd of 6 suports
Bridge ID #	Structure #3
Sample ID #	289/6282/SB 3-3/1 289/6282/SB 3-3/1.5 289/6282/SB 3-3/2
Sample Location: 22 feet above the ground on the west face of the column.	**Comments:** ➢ Severe cracking and staining longitudinally along column. ➢ Chloride samples taken just above that point where the column diameter is reduced (at 22' above ground). ➢ Drilling depth exceeds 2" due to concrete spalling.
Concrete Surface Description: ➢ Stained and damp-looking. ➢ Severe cracking. ➢ Some corrosion stains. ➢ Bent above column is spalling (delamination).	

Chloride Sample Data Sheet Project 1774 Sheet ___6___	
Date	7-1-98
Weather Condition	Windy – clear skies.
Bridge Location	289/MD/EB
Bridge ID #	Structure #2
Sample ID #	289/MD/EB6/17/1 289/MD/EB6/17/1.5 289/MD/EB6/17/2
Sample Location: About 17 feet from downstream end.	**Comments:**
Concrete Surface Description:	

Chloride Sample Data Sheet Project 1774 Sheet ___7___	
Date	7-1-98
Weather Condition	Windy, warm – getting cloudy.
Bridge Location	289/MD/EB
Bridge ID #	Structure #2
Sample ID #	289/MD/EB6/25/1 289/MD/EB6/25/1.5 289/MD/EB6/25/1
Sample Location: Immediately left of center column, about 25 feet from the downstream end.	**Comments:**
Concrete Surface Description:	

Chloride Sample Data Sheet Project 1774 Sheet ___8___	
Date	7-1-98
Weather Condition	Windy, some rain.
Bridge Location	289/MD/WB
Bridge ID #	Structure #1
Sample ID #	289/MD/WB2/1 289/MD/WB2/1.5 289/MD/WB2/2
Sample Location:	**Comments:**
Concrete Surface Description: ➢ Same area that was ground for corrosion rate testing.	

Chloride Sample Data Sheet Project 1774 Sheet ___9___	
Date	7-1-98
Weather Condition	Windy and cloudy.
Bridge Location	6282/Mainlane Overpass
Bridge ID #	Structure #5
Sample ID #	62821/WB1/1 62821/WB1/1.5 62821/WB1/2
Sample Location:	**Comments:**
Concrete Surface Description:	

Chloride Sample Data Sheet Project 1774 Sheet ___10___	
Date	7-1-98
Weather Condition	Windy and cloudy.
Bridge Location	6282/Mainlane Overpass
Bridge ID #	Structure #5
Sample ID #	62821/WB1/b/1 62821/WB1/b/1.5 62821/WB1/b/2
Sample Location: On spalled side of bent.	**Comments:**
Concrete Surface Description:	

Chloride Sample Data Sheet Project 1774 Sheet ___11___	
Date	7-2-98
Weather Condition	Warm and sunny, a bit cloudy.
Bridge Location	US84/FM41EB
Bridge ID #	Structure #10
Sample ID #	US84/FM41/EB1/1 US84/FM41/EB1/1.5 US84/FM41/EB1/2
Sample Location:	**Comments:**

Concrete Surface Description:

- Very thick coating on surface with a grainy, rough texture.
- Some repair patches.

Chloride Sample Data Sheet Project 1774 Sheet ___12___	
Date	7-2-98
Weather Condition	Windy, overcast, and warm.
Bridge Location	US84/FM400/EB
Bridge ID #	Structure #11
Sample ID #	US84/FM400/EB2/1 US84/FM400/EB2/1.5 US84/FM400/EB2/2
Sample Location: Drilling done on top of bent.	**Comments:**
Concrete Surface Description:	

Appendix E

PERMEABILITY DATA SHEETS

Permeability Measurement (SAF Device) Data Sheet Project 1774 Sheet __1__	
Date	6-30-98
Bridge Location **(Lubbock, TX)**	6282 Eastbound at 289 – 6282/289/EB
Bridge ID #	Structure #8
Sample ID #	6282/289/EB5
Sample Location: East side, 10 feet from downstream end- right of exterior column.	**Comments:** ➢ VAC stabilized at 686.
Concrete Surface Description: ➢ Brush ridges on the paint/sealer surface.	
Flow Reading	18.51
Vacuum Reading	683.3
RPT Core ID #	6282/289/EB5
Half-Cell Potential (mV vs. Cu-$CuSO_4$)	915

Permeability Measurement (SAF Device) Data Sheet Project 1774 Sheet 2	
Date	6-30-98
Bridge Location **(Lubbock, TX)**	6282/289/WB1
Bridge ID #	Structure #7
Sample ID #	6282/289/WB1
Sample Location:	**Comments:** ➢ Severe delamination on top of bent.
Concrete Surface Description: ➢ Concrete surface was dirty before grinding..	
Flow Reading	71.08
Vacuum Reading	678.3
RPT Core ID #	6282/289/WB1
Half-Cell Potential (mV vs. Cu-$CuSO_4$)	54

Permeability Measurement (SAF Device) Data Sheet Project 1774 Sheet __3___	
Date	7-1-98
Bridge Location **(Lubbock, TX)**	289/MD/EB
Bridge ID #	Structure #2
Sample ID #	289/MD/EB6
Sample Location: Just to the right of the core.	**Comments:** ➢ Initial vacuum = 685.
Concrete Surface Description:	
Flow Reading	97.45
Vacuum Reading	666.4
RPT Core ID #	289/MD/EB6
Half-Cell Potential (mV vs. Cu-$CuSO_4$)	None.

Permeability Measurement (SAF Device) Data Sheet Project 1774 Sheet 4	
Date	7-2-98
Bridge Location **(Lubbock, TX)**	US 84 and FM 41 (Eastbound traffic) – 84/41/EB
Bridge ID #	Structure #10
Sample ID #	84/41/EB1
Sample Location:	**Comments:** ➢ Initial vacuum = 690.
Concrete Surface Description:	
Flow Reading	43.5
Vacuum Reading	687.6
RPT Core ID #	84/41/EB1
Half-Cell Potential (mV vs. Cu-$CuSO_4$)	55

Appendix F

SAMPLE OF PR MONITOR DATA FILE

BEAM 1.1 MIDSPAN
PR

[COMMENT]
beam1-1midspan

[SETUP]
Setup name, beam1
Number of tests,1
Minutes between tests,10
Step Duration,15
Step Size,22.706385
Initial scan potential,-68
Final scan potential,68
Drift choice,0
Measurement units,1
Electrode area,38.520000
Environment constant,0.026000
Material Index,0
Material constant,11619.000000
Material name,Iron Number of test stations,1

[TESTNUMBER]
1

[RESULTS]
Total DC resistance, 3813
Solution resistance, 2904
Polarization resistance, 909
Corrosion rate, 0.053
Free Corrosion Potential,-0.1614
Linear regression coefficient,0.9999

[DRIFT]
0
0
0
0

[BADPOINTS]
0
0
0
0

[SCANDATA]
Potential,Noise,Current
-229.86,0.000312548, -17.31
-206.81,0.000315107, -10.58
-183.97,0.000315464, -4.43
-161.14,0.000312935,   1.82
-138.40,0.000313180,   7.52
-116.10,0.000316850, 13.43
 -92.51,0.000314026, 19.41
[ENDSCAN]

Appendix G

OUTLINE OF LABORATORY RESEARCH PROGRAM

G.1 Specimen Parameters and Construction Practices

The parameters considered in the laboratory program include:

- Specimen geometry,
- Chloride content in concrete mix,
- Cracking condition,
- Type of repair material,
- Condition (wet or dry) of the wrapped surface below the waterline,
- Application of corrosion inhibitor,
- Type of wrapping system,
- Length of wrapped surface.

Specimen Geometry

Two specimen shapes are considered for this study: circular and rectangular. Specimens with circular cross-sections were cast to represent a typical column or pier design. The dimensions of these sections are 10-in. diameter x 36-in. long. The reinforcement for each specimen consists of four No. 6 bars in the longitudinal direction and nine circular ties made from ¼-in. plain wire and spaced at four inches as transverse reinforcement. The reinforcement cages were assembled to provide 1 in. of concrete cover along the sides and bottom of the specimen. Conventional tie-wire was used in the construction of the cages. The 1-in. cover was maintained during casting by reinforcement chairs placed inside the form. Plastic chairs were used in lieu of

metal chairs that may corrode and distort the evaluation during the monitoring schedule.

The rectangular specimens are 10-in. x 10-in. x 36-in. and are meant to simulate bridge beams. They are reinforced with four No. 6 bars longitudinally and three bent U-shaped stirrups transversely. The stirrups are ¼-in. plain wire; cold-worked into shape. As with the circular specimens, plastic chairs were used to provide a 1 in. concrete cover on all sides and standard tie-wire was employed for construction.

Chloride Content in the Concrete Mix

To investigate the effect of residual chlorides in a repaired and wrapped section, approximately half of the sections were cast with a concrete mix containing chlorides. An identical mix, without chlorides, was used in the remainder of the specimens. This basic concrete mix design is shown in Table G.1.

Table G.1 Concrete Mix Design.

Item	Amount (lbs./yd^3)
Cement	393
Coarse Ag. (3/4-in. Crushed Limestone)	1970
Fine Ag. (Colorado River Sand)	1620
Water	275

The resulting water-cement ratio of about 0.7 is purposely high to produce a relatively permeable concrete matrix that will accelerate corrosion.

Salt was added to the portion of the mix meant for residual chloride exposure. The salt was dissolved in water, which was subsequently added to the batched mix. The amount of water used for dissolution was deliberately withheld from the batched mix to keep the water content consistent. Salt addition was proportioned at 3.5 percent by weight of the mix water. This results in a chloride content of about 0.23 percent by weight for the entire mix.

Cracking Condition

Cracking is an important variable to consider when investigating corrosion in reinforced concrete. Cracks provide access by the chlorides to the steel, accelerating and localizing exposure. Cracks may be present for many reasons including tensile stresses and the presence of internal pressures from previous corrosion reactions inside the concrete. For these reasons, some of the specimens are intentionally cracked prior to repair, wrap, and exposure. This simulates the conditions observed in structures subjected to corrosive environments; even after repair work has been done.

Specimens were loaded to achieve a crack width on the order of 0.01-0.013 in. This corresponds to the maximum crack width allowed for exterior exposure by ACI 10.6.4 (ACI 1995). The cracking was done by load application using a Universal Testing Machine (UTM). Rectangular sections were subjected to flexural load, producing tensile cracks on the bottom portion of the member. Circular specimens were loaded in flexure on opposing sides, to produce cracks through the member. Due to the small span-to-depth ratios during loading, many of the cracks show some characteristics of flexure/shear interaction and the arching action common in deep beams.

Type of Repair Material

Because the removal and replacement of damaged concrete is common in repair for corrosion damage, two commonly used repair materials approved by the Texas Department of Transportation (TXDOT) were investigated. The materials used are a latex-modified concrete (Sikadur 42) and an epoxy-modified grout (SikaTop 122 Plus). Twenty specimens contain repair material in the region exposed to corrosive elements.

The repair materials were applied after the specimens were cracked. Concrete cover was removed with a chipping hammer to the level of the longitudinal reinforcement. After cover removal, the specimens to be repaired were formed with metal flashing or plywood and the repair materials were then applied to regain the original dimensions of the members. Much of the repair material was allowed to flow into place, with external vibration aiding the consolidation. The remainder of the material was placed by dry-packing.

Surface Condition

Exterior wrap can be applied below the waterline on a pier element. This requires wrap application on a wet surface. To simulate this situation, four of the circular specimens were immersed in saltwater immediately prior to wrapping. The adherence of the wrap and the use of a different epoxy curing agent than is commonly applied to dry surfaces are also evaluated.

Application of Corrosion Inhibitor

The application of corrosion inhibitors to the exterior of repaired elements in corrosive environments is becoming more common as new products are produced. One such product, Sika Ferrogard 903, was applied to the surface

of 16 specimens before the wrap was applied. The inhibitor is watery in texture and was applied with a conventional paint-roller.

Type of Wrapping System

To evaluate the effect of the type of wrapping system on the corrosion characteristics of a member, three distinct systems are considered – one proprietary system and two different generic systems. A system consists of a fabric and a resin and curing agent to be mixed and saturated into the fabric.

The proprietary system is the Tyfo® S Fibrwrap® system developed and provided by Delta Structural Technology, Inc. This system has been used in a variety of strengthening applications, and is currently being applied on project CSR 783-2-66 in Lubbock, TX to provide corrosion protection. Fibrwrap® is being used on 15 of the specimens in the laboratory program.

The generic systems developed for this study use the same fabric, but have different resins. One system uses an epoxy resin, as does the Fibrwrap® system, and the other system has a vinyl-ester resin component. The generic systems will be compared with the proprietary system and with each other to assess the corrosion protection offered. The fabric used for the generic systems is not as substantial as the fabric used in the proprietary system. The generic fabric is thinner and the mesh is not as strong.

For comparison and control purposes, 16 of the specimens were not wrapped, but will be exposed to the same corrosive conditions as the others.

Length of Wrapped Surface

The length of the wrap is a variable to study the effect of different exposed surface areas in the circular (pier application) specimens. The wrap length for the rectangular (endcap exposure) specimens was kept constant at about 27 to 30 in. from the downstream end and is not a variable for these members. Three different wrap lengths are considered for the circular sections (all are measured from the top of the specimen down toward the base): 24 in., 30 in., and 36 in. or full wrap. The 24-in. length represents a wrap extending to the waterline. The 30-in. wrap extends below the waterline and represents specimens wrapped with the wet surface condition. The 36-in. wrap encloses the entire surface in an attempt to completely prevent chloride ingress along the length of the specimen. Even on the fully wrapped members the bottom surface is not wrapped to better represent field conditions, where the end of the pier is a foundation or the sea bed. Examples of specimens with the 24-in. and 36-in wraps are shown in Figure G.1.

Figure G.1 Specimens of different wrap lengths.

G.2 Exposure Conditions

The purpose of the exposure environment is to simulate common field exposures while accelerating the corrosion condition. This requires two distinct types of exposure conditions – one for the circular specimens and one for the rectangular specimens.

The circular specimens are representative of submerged pier elements in a marine environment. These elements are immersed in saltwater to a depth of 12 in. during the wet cycles of the exposure program. During the dry cycles, the water level is lowered below the bottom of the specimens. The circular specimens are shown in Figure G.2 as they rest in the immersion pool.

The rectangular specimens are exposed in a situation replicating the downstream endcap of a bridge beam. To achieve this condition, water is distributed along all sides on the enclosed end of the specimens during the wet cycles. The members are set at an angle to promote saltwater flow toward the enclosed end. The exposure environment of the rectangular specimens is shown in Figure G.3.

Figure G.2 The exposure environment for the circular specimens.

Figure G.3 The exposure environment for the rectangular specimens.

All of the specimens in the exposure study are contained in the same water-tight pool. The pool is constructed of wooden walls attached to all four sides of an elevated slab and lined with layers of plastic. Saltwater is transported into and out of the pool using a pump connected to a piping system. During the

wet cycles, the pump also transports saltwater through pipes to the tops of the beam elements. The saltwater flows from the pipes onto the beams through pre-drilled holes. During the dry cycles, the saltwater is stored in a galvanized steel tank for reuse. The saltwater used for this corrosive environment is 3.5% salt by weight.

The cyclic wet/dry exposures will be repeated continuously for the length of the study with one week wet, two weeks dry.

G.3 Performance Monitoring Program

During the life of the corrosion study, the specimens will be consistently monitored for corrosion potential. Monitoring is carried out by taking half-cell potential measurements once every two full wet/dry cycles.

To provide a connection to the working electrode (corroding surface), the longitudinal reinforcement is extended out of the concrete on one end of each specimen. The electrical connection is supplied by a lead wire attached to a brass fastener, which is in turn attached to the exposed reinforcement (this can be seen in Figure G.2). The exposed bars are protected from the corrosive environment by the application of grease to the steel surface.

Corrosion potential measurements are procured with a saturated calomel electrode. This reference electrode and the working electrode are circuited into a voltmeter to measure the potential differential.

To prevent any interference with the wrap below the waterline, the electrode is applied at a distance of 16 in. from the bottom of the circular specimens (4 in. above the waterline). Measurements are taken on the downstream end-section of the rectangular specimens. On wrapped specimens, contact with the concrete surface for electrode application is established by removal of the wrap in a 1 ¼-in diameter area. These sections are replaced by water-tight, removable tabs which require resealing after each set of measurements is taken.

Bibliography

American Concrete Institute. (1995). Building Code Requirements for Structural Concrete (ACI 318-95) and Commentary (ACI 318R-95), American Concrete Institute, Farmington Hills, MI.

American Concrete Institute Committee 222. (1991). "Corrosion of Metals in Concrete," ACI 222R-85, ACI Manual of Concrete Practice, Part I, American Concrete Institute, Detroit, MI.

ASTM. (1998). "Standard Test Method for Half-Cell Potentials of Uncoated Reinforcing Steel in Concrete," Annual Book of ASTM Standards, Designation: C 876-91, ASTM, West Conshohocken, PA, 430-435.

ASTM. (1998). "Standard Test Method for Electrical Indication of Concrete's Ability to Resist Chloride Ion Penetration," Annual Book of ASTM Standards, Designation: C 1202-97, ASTM, West Conshohocken, PA, 622-627.

Broomfield, J. P. (1997). Corrosion of Steel in Concrete, E. & F.N. Spon, London, UK.

Buzbee, Sally. (1994). "Freeway material resists quakes," Associated Press, 1994.

Civil Engineering. (1994). "Fiber Wraps Migrate East," Civil Engineering, July 1994.

Concorr. (1998). “Corrosion Rate Probe and Connection Details,” Concorr, Inc., Ashburn, VA.

Cortest Instrument Systems, Inc. Operating Manual for the PR Monitor Version 5.00, Cortest Instrument Systems, Inc., Willoughby, OH.

Delta Structural Technology, Inc. (1998). Composite Fiberwrap, Delta Structural Technology, Inc., Humble, TX.

Fraczek, John. (1987). “A Review of Electrochemical Principals as Applied to Corrosion of Steel in a Concrete of Grout Environment,” Corrosion, Concrete, and Chlorides. Steel Corrosion in Concrete: Causes and Restraints, American Concrete Institute, (SP-102-1), Detroit, MI, 13-24.

Francois, R., and Arliguie, G. (1991). “Reinforced Concrete: Correlation Between Cracking and Corrosion,” Durability of Concrete, Second International Conference, Volume II, (SP 126-65), American Concrete Institute, Detroit, MI, 1221-1238.

Fuentes, Laura Alexandra. (1999). “Implementation of Composite Wrapping Systems on Reinforced Concrete Structures Exposed to a Corrosive Laboratory Environment,” Thesis, Civil Engineering Department, University of Texas at Austin, 1999.

Hausmann, D. A. (1964). “Electrochemical Behavior of Steel in Concrete,” Journal of the ACI, (February 1964), American Concrete Institute, Detroit, MI, 171-187.

Hime, W., and Erlin, B. (1987). "Some Chemical and Physical Aspects of Phenomena Associated with Chloride-Induced Corrosion," Corrosion, Concrete, and Chlorides. Steel Corrosion in Concrete: Causes and Restraints, American Concrete Institute, (SP-102-1), Detroit, MI, 1-12.

James Instruments Inc. The Gecor6 Corrosion rate Meter for Steel in Concrete, James Instruments Inc., Chicago, IL.

Jones, Denny A. (1996). Principles and Prevention of Corrosion, Second Edition, Prentice Hall, Upper Saddle River, NJ.

Kenneth C. Clear, Inc. (1990). KCC Inc. 3LP Package Test Procedures, Data Analysis Procedures and General Information, Kenneth C. Clear, Inc., Sterling, VA, July 1990.

Master Builders Technologies. (1999). masterbuilders.com/struct.htm

McConnell, Vicki P. (1993). "Bridge Column Retrofit," High Performance Composites, September/October 1993, 62-64.

Mirmiran, Amir. (1997). "FRP-Concrete Composite Column and Pile Jacket Splicing Phase II," Department of Civil & Environmental Engineering, University of Central Florida, August 1997.

Mirsa, S., and Uomoto, T. (1991). "Reinforcement Corrosion Under Simultaneous Diverse Exposure Conditions," Durability of Concrete, Second International Conference, Volume I, (SP 126-22), American Concrete Institute, Detroit, MI, 423-442.

Mufti, Aftab A., Erki, Marie-Anne, and Jaeger, Leslie G. (1991). "Chapter 1: Introduction and Overview," Advanced Composite Materials with Applications to Bridges, The Canadian Society for Civil Engineering, Montreal, P.Q., Canada, 1-20.

Neale, K. W., and Labossiere, P. (1991). "Chapter 2: Material Properties of Fibre-Reinforced Plastics," Advanced Composite Materials with Applications to Bridges, The Canadian Society for Civil Engineering, Montreal, P.Q., Canada, 21-69.

Okpala, Daniel. (1996). Correspondence with Mathew Murphy, August 1996.

Roper, H., and Baweja, D. (1991). "Carbonation-Chloride Interactions and Their Influence on Corrosion Rates of Steel in Concrete," Durability of Concrete, Second International Conference, Volume I, (SP 126-22), American Concrete Institute, Detroit, MI, 295-316.

Saadatmanesh, Hamid, and Ehsani, Mohammed R. (1996). "Experimental Study of Concrete Girders Rerofitted with Epoxy-Bonded Composite Laminates," Repair and Strengthening of Concrete Members with

Adhesive Bonded Plates, (SP 165) American Concrete Institute, Farmington Hills, MI, 205-234.

Saadatmanesh, Hamid, Ehsani, Mohammed R., and An, Wei (1996). "Analytical Study of Concrete Girders Rerofitted with Epoxy-Bonded Composite Laminates," Repair and Strengthening of Concrete Members with Adhesive Bonded Plates, (SP 165) American Concrete Institute, Farmington Hills, MI, 235-259.

Scannell, William T., Sohanghpurwala, Ali A., and Islam, Moavin. (1996). "Assessment of Physical Condition of Concrete Bridge Components," FHWA-SHRP Showcase Participant's Workbook, Concorr, Inc., Ashburn, VA, 1996.

Sheikh, S., Pantazopoulou, S., Bonacci, J., Thomas, M., Hearn, N. "Repair of Delaminated Circular Pier Columns by ACM," Ontario Joint Transportation Research Report, MTO Reference Number 31902.

Sohanghpurwala, Ali Akbar, and Scannell, William T. (1994). "Repair and Protection of Concrete Exposed to Seawater," Concrete Repair Bulletin, July/August 1994, 8-13.

Swamy, R. N. (1990). "Durability of Rebars in Concrete," Durability of Concrete, G.M. Idorn International Symposium, (SP 131-3), American Concrete Institute, Detroit, MI, 67-98.

Unal, Muhammed A., and Jirsa, James O. (1998). “Evaluation of an Encapsulation and Epoxy Resin Injection Procedure for Rehabilitating Corroding Reinforced Concrete Structures,” PMFSEL Report 98-3, Ferguson Laboratory, The University of Texas at Austin, September 1998.

United States Census Bureau. (1999). state.tx.us/maps/303.html

Vaca, Enrique Cortes. (1993). “Electrochemical Procedures to Rehabilitate Corroded Concrete Structures,” Departmental Report, University of Texas at Austin, May 1993.

West, J. (1999). “Durability Design of Post-Tensioned Bridge Substructures,” Dissertation, Civil Engineering Department, University of Texas at Austin, 1999.

XXsys Technologies, Inc. (1998). “Automated Column Wrapping Process Overview,” XXsys Technologies, Inc. San Diego, CA, 1998.

Yeomans, S. R. (1991). “Comparative Studies of Galvanized and Epoxy Coated Steel Reinforcement in Concrete,” Durability of Concrete, Second International Conference, Volume I, (SP 126-19), American Concrete Institute, Detroit, MI, 355-370.